Annual Reviews of Astronomy and Astrophysics 2006 – 44: xxx




# STELLAR POPULATION DIAGNOSTICS OF ELLIPTICAL GALAXY FORMATION

*Alvio Renzini*
INAF, Osservatorio Astronomico di Padova

KEYWORDS: galaxy formation, galaxy evolution, galaxy surveys, stellar populations

**ABSTRACT:**
Major progress has been achieved in recent years in mapping the properties of passively-evolving, early-type galaxies (ETG) from the local universe all the way to redshift $\sim 2$. Here, age and metallicity estimates for local cluster and field ETGs are reviewed as based on color-magnitude, color-$\sigma$, and fundamental plane relations, as well as on spectral-line indices diagnostics. The results of applying the same tools at high redshifts are then discussed, and their consistency with the low-redshift results is assessed. Most low- as well as high-redshift ($z \sim 1$) observations consistently indicate 1) a formation redshift $z \gtrsim 3$ for the bulk of stars in cluster ETGs, with their counterparts in low-density environments being on average $\sim 1-2$ Gyr younger, i.e., formed at $z \gtrsim 1.5-2$; 2) the duration of the major star formation phase anticorrelates with galaxy mass, and the oldest stellar populations are found in the most massive galaxies. With increasing redshift there is evidence for a decrease in the number density of ETGs, especially of the less massive ones, whereas existing data appear to suggest that most of the most-massive ETGs were already fully assembled at $z \sim 1$. Beyond this redshift, the space density of ETGs starts dropping significantly, and as ETGs disappear, a population of massive, strongly clustered, starburst galaxies progressively becomes more and more prominent, which makes them the likely progenitors to ETGs.

CONTENTS

## 1 INTRODUCTION

Following Hubble (1936), we still classify galaxies as ellipticals, spirals and irregulars (see Sandage 2005, and references therein). This was an eyeball, purely morphological scheme; however, morphology correlates with the stellar population content of these galaxies, with typical ellipticals being redder than the others, and showing purely stellar absorption-line spectra with no or very weak nebular emissions. As a consequence, one often refers to early-type galaxies (ETG), even if they are color (or spectral type) selected rather than morphologically selected. Furthermore, the bulges of spirals of the earlier types show morphological as well as spectral similarities with ellipticals, and one often includes both ellipticals and bulges under the category of galactic spheroids.

Morphologically-selected and color-, or spectrum-selected samples do not fully overlap. For example, in a recent study of local ($z \sim 0$) ETGs from the Sloan Digital Sky Survey (SDSS) all three criteria were adopted (Bernardi et al. 2006), and the result is reported in Table 1 (M. Bernardi, private communication).[1] From a sample including ∼123,000 galaxies with $14.5 < r_{\rm Petrosian} < 17.77$ and $0.004 < z < 0.08$, ETGs have been selected in turn by each of the three criteria (MOR, COL, SPE), and the resulting numbers of galaxies fulfilling each of them is given on the diagonal of the matrix. Out of the diagonal are the fractions of galaxies that satisfy two of the criteria, as labelled in the corresponding row and column. So, out of the morphologically-selected ETGs, 70% satisfy also the color selection, etc. The correlation between color and morphology selection persists at high redshift, e.g., at $z \sim 0.7$ about 85% of color-selected, red-sequence galaxies are also morphologically early-type, i.e., E/S0/Sa (Bell et al 2004a), an estimate broadly consistent with the local one, when allowing for the wider morphological criterion.

**Table 1.** Morphology- Versus Color- Versus Spectrum-Selected Samples

| | MOR | COL | SPE |
|---|---|---|---|
| MOR | 37151 | 70% | 81% |
| COL | 58% | 44618 | 87% |
| SPE | 55% | 70% | 55134 |

It is estimated that true ellipticals represent ∼ 22% of the total mass in stars in the local universe, a fraction amounting to ∼ 75% for spheroids (i.e., when including E0's and spiral bulges), whereas disks contribute only ∼ 25% and dwarfs an irrelevant fraction (Fukugita, Hogan, & Peebles 1998). Although earlier estimates gave slightly lower fractions for stars in spheroids vs. disks (e.g. Schechter & Dressler 1987; Persic & Salucci 1992), it is now generally accepted that the majority of stars belong to spheroids. Figure 1 shows separately the mass functions of color-selected ETGs and of blue, star-forming galaxies, also based on the SDSS data (Baldry et al. 2004). Above $\sim 3 \times 10^{10} M_\odot$ red-sequence galaxies start to increasingly outnumber blue galaxies by a factor that exceeds 10 above $\sim 3 \times 10^{11} M_\odot$. Figure 2, drawn from the same mass functions, shows the contributions to the total stellar mass by red and blue galaxies in the various mass bins, along with the contributions to the total number of galaxies. Then, ETGs

[1]Here, as well as through the whole paper, the definition of the specific criteria adopted by the various authors for their sample selections can be found in the original articles.

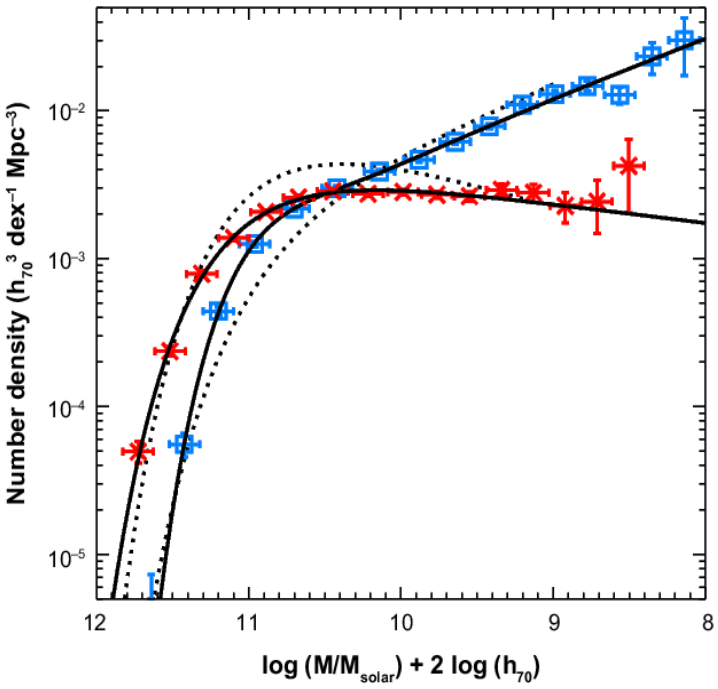


Figure 1: The mass function of local ($z \sim 0$) early-type (red) galaxies and late-type (blue) galaxies from the Sloan Digital Sky Survey (Baldry et al. 2004). The solid lines represent best fit Schechter functions. For the blue galaxies the sum of two different Schechter functions is required to provide a good fit. Dotted lines show the mass functions from Bell et al. (2003).

represent only 17% of the total number of galaxies in the sample, but contribute $\sim 57\%$ of the total mass. Moreover, $\gtrsim$80% of the stellar mass in ETGs belongs to galaxies more massive than $\sim 3 \times 10^{10} M_{\odot}$. Dwarfs are sometimes seen as the "building blocks" of galaxies, but at least in the present universe one can not build much with them.

With spheroids holding the major share of stellar mass in galaxies, understanding their evolution – from formation to their present state – is central to the galaxy evolution problem in general. Historically, two main scenarios have confronted each other, the so-called Monolithic Collapse model (Eggen, Lynden-Bell & Sandage 1962, Larson 1974, Arimoto & Yoshii 1987, Bressan, Chiosi & Fagotto 1994), and the Hierarchical Merging model (e.g., Toomre 1977; White & Rees 1978). In the former scenario spheroids form at a very early epoch as a result of a global starburst, and then passively evolve to the present. If the local conditions are appropriate, a spheroid can gradually grow a disk by accreting gas from the environment, hence spheroids precede disks. In the merging model, big spheroids result from the mutual disruption of disks in a merging event, hence disks precede spheroids.

The two scenarios appear to sharply contradict each other, but the contradiction has progressively blurred in recent years. Evidence has accumulated that the bulk of stars in spheroids are old, and most likely formed in major merging events. In the hierarchical merging scenario (the only one rooted in a solid cosmological context) successive generations of models have struggled to increase their predicted stellar ages, so as to produce results resembling the opposite sce-

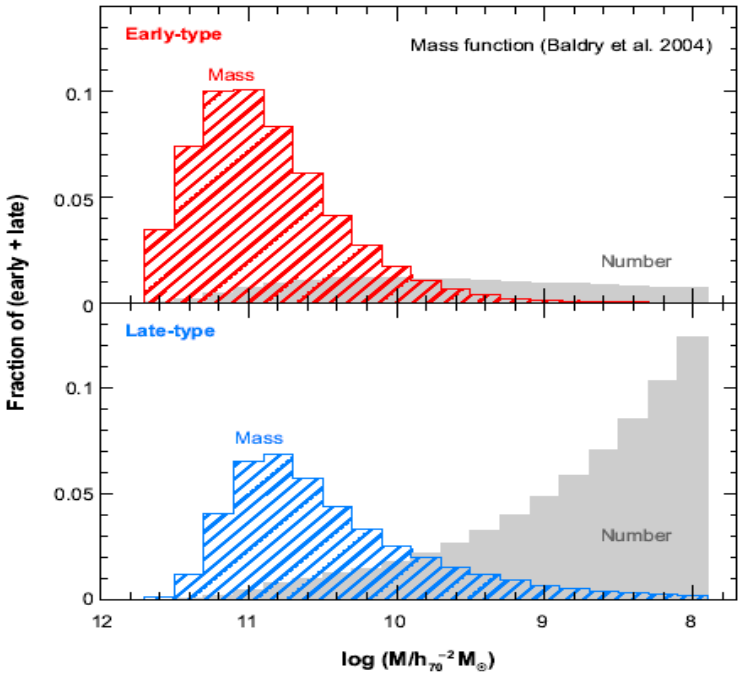


Figure 2: The contributions to the total stellar mass and to the number of galaxies by early-type (red) and late-type (blue) galaxies in the various mass bins, as derived from the best-fit mass functions of Baldry et al. (2004) shown in Figure 1. The relative areas are proportional to the contributions of the early- and late-type galaxies to the total stellar mass and to the number of galaxies. (Courtesy of D. Thomas).

nario. This review will not attempt to trace an history of theoretical efforts to understand the formation and evolution of ellipticals and spheroids. It will rather concentrate on reviewing the accumulating observational evidences coming from the stellar component of these galaxies. Other extremely interesting properties of ellipticals, such as their structural and dynamical properties, their hot gas content, central supermassive black holes, etc., will not be touched in this review, even if they are certainly needed to complete the picture and likely play an important role in the evolution of these galaxies. Also untouched are the internal properties of ETGs, such as color and line-strength gradients indicative of spatial inhomogeneities of the stellar populations across the body of ETGs. A complementary view of ETG formation based on the globular cluster populations of these galaxies is presented in the article by J. Brodie & J. Strader (this volume).

The "concordance cosmology" ($\Omega_{\rm M} = 0.3,\ \Omega_\Lambda = 0.7,\ H_\circ = 70$) is adopted if not explicitly stated otherwise.

## 2 SYNTHETIC STELLAR POPULATIONS

The ETGs treated in this review can only be studied in integrated light, hence the interpretation of their photometric and spectroscopic properties needs population synthesis tools. Pioneering unconstrained synthesis using "quadratic programming" (e.g., Faber 1972), was soon abandoned in favor of evolutionary population synthesis, whose foundations were laid down by Beatrice Tinsley in the

1970s (Tinsley & Gunn 1976, Tinsley 1980, Gunn, Stryker & Tinsley 1981). Much progress has been made in the course of the subsequent quarter of a century, especially thanks to the systematic production of fairly complete libraries of stellar evolutionary sequences and stellar spectra.

Several modern population synthesis tools are commonly in use today, including those of Worthey (1994), Buzzoni (1995), Bressan, Chiosi, & Tantalo (1996), Maraston (1998, 2005), Bruzual & Charlot (2003), Fioc & Rocca Volmerange (1997, PEGASE Code), Vázques & Leitherer (2005, Starburst99 Code), Vazdekis et al. (2003), and González Delgado et al. (2005). Though far more reliable than earlier generations of models, even the most recent tools still may suffer from incomplete spectral libraries (especially at high metallicity and for nonsolar abundance ratios), and poorly calibrated mass loss in advanced stages, such as the asymptotic giant branch (AGB). Yet, there is fair agreement among the various models, with the exception of those for ages around $\sim 1$ Gyr, when the contribution by AGB stars is at maximum, and Maraston's models (calibrated on Magellanic Cloud clusters) give appreciably higher near-IR fluxes than the other models.

Only a few "rules of thumb" regarding population synthesis models can be recalled here, which may be useful in guiding the reader through some of the subtleties of their comparison with the observations.

- No evolutionary population synthesis code is perfect. Evolutionary tracks are not perfect and stellar libraries are never really complete. So, any code deficiency will leave its imprint on the results, generating a distortion of the age/metallicity grids used to map plots of one observable versus another. Inevitably, such distortions will leave their imprint in the results, and to some extent may lead to spurious correlations/anticorrelations when reading ages and metallicities from overplotted data points.
- Ages derived from best fits to simple stellar populations (SSPs, i.e., single burst populations) are always luminosity-weighted ages, and in general are more sensitive to the youngest component of the real age distribution. SSP ages should be regarded as lower limits.
- Spectra and colors of SSPs are fairly insensitive to the initial mass function (IMF), because most of the light comes from stars in a narrow mass interval around the mass of stars at the main sequence turnoff.
- The time evolution of the luminosity of a SSP does depend on the IMF, and so does the mass-to-light ratio ($M/L$). For example, a now fashionable IMF that flattens below $\sim 0.6\,M_\odot$ (e.g., Chabrier 2003) gives $M/L$ ratios a factor of $\sim 2$ lower than a straight Salpeter IMF.
- Stellar ages and metallicities are the main quantities that the analyses of colors and integrated spectra of galaxies are aimed to determine. Yet, for many observables, age and metallicity are largely degenerate, with a reduced age coupled to an increased metallicity conjuring to leave the spectral energy distribution nearly unchanged. This results primarily from the color (temperature) of the main sequence turnoff, e.g., $(B-V)^{\rm TO}$, (the true clock of SSPs) being almost equally sensitive to age and metallicity changes. Indeed, from stellar isochrones one can derive that $(\partial \log\, t/\partial[{\rm Fe/H}])_{(B-V)^{\rm TO}} \simeq -0.9 - 0.35[{\rm Fe/H}]$, and a factor of 2 error in estimated metallicity produces a factor $\sim 2$ error in age (Renzini 1992). Red giant branch stars are the major contributors of bolometric luminosity in old stellar populations, and their locus shifts to lower temperatures with both increasing age and metallicity, further contributing to the degeneracy. Thus, from full SSPs,

Worthey (1994) estimated that a factor of 3 error in metallicity generates a factor of 2 error in age when using optical colors as age indicators, the so-called 2/3 rule. Several strategies have been devised to circumvent this difficulty and break the age-metallicity degeneracy (see below).

• There are occasionally ambiguities in what is meant by the $M/L$ ratio in the tabulated values. The mass $M$ can be defined either as the mass of gas that went into stars, or the mass of the residual population at age $t$, including the mass in dead remnants (i.e., the original mass diminished by the mass lost by stars in the course of their evolution), or even the mass of the surviving stars, i.e., without including the mass in remnants. Caution should be paid when using tabular values, as different authors may adopt different definitions.

The power of stellar population diagnostics stems from the opportunity to age-date the stellar content of galaxies in a fashion that is independent of cosmological parameters. Then, once a cosmology is adopted, ages derived from observations at a lower redshift can be used to predict the properties of the stellar populations of ETGs at a higher one, including their formation redshift. Thus, ages derived for the local elliptical galaxies imply a well-defined color, spectral, and luminosity evolution with redshifts, which all can be subject to direct observational test. The extent to which a consistent picture of ETG formation is emerging from low- and high-redshift observations is the main underlying theme of this review.

## 3 ELLIPTICAL GALAXIES IN THE LOCAL UNIVERSE

Observations at high redshift are certainly the most direct way to look at the forming galaxies, and a great observational effort is currently being made in this direction. Yet, high-redshift galaxies are very faint, and only few of their global properties can now be measured. Nearby galaxies can instead be studied in far greater detail, and their fossil evidence can provide a view of galaxy formation and evolution that is fully complementary to that given by high-redshift observations. By fossil evidence one refers to those observables that are not related to ongoing, active star formation, and which are instead the result of the integrated past star formation history. At first studies attempted to estimate ages and metallicities of the dominant stellar populations on a galaxy-by-galaxy basis. But the tools used were still quite rudimentary, being based on largely incomplete libraries of stellar spectra and evolutionary sequences. Hence, through the 1980s progress was relatively slow, and opinions could widely diverge as to whether ellipticals were dominated by old stellar populations –as old as galactic globular clusters– or by intermediate age ones, several billion years younger than globulars (see e.g. O'Connell 1986, Renzini 1986) –with much of the diverging interpretations being a result of the age-metallicity degeneracy. From the beginning of the 1990s progress has been constantly accelerating, and much of this review concentrates on the developments that took place over the past 15 years.

### *3.1 Color-Magnitude Relation, Fundamental-Plane and Line-Indices*

3.1.1 THE COLOR-MAGNITUDE AND COLOR-$\sigma$ RELATIONS That elliptical galaxies follow a tight color-magnitude (C-M) relation was first recognized by Baum (1959), and in a massive exploration Visvanathan & Sandage (1977) and Sandage & Visvanathan (1978a,b) established the universality of this relation with what continues to be the culmination of ETG studies in the pre-CCD era.

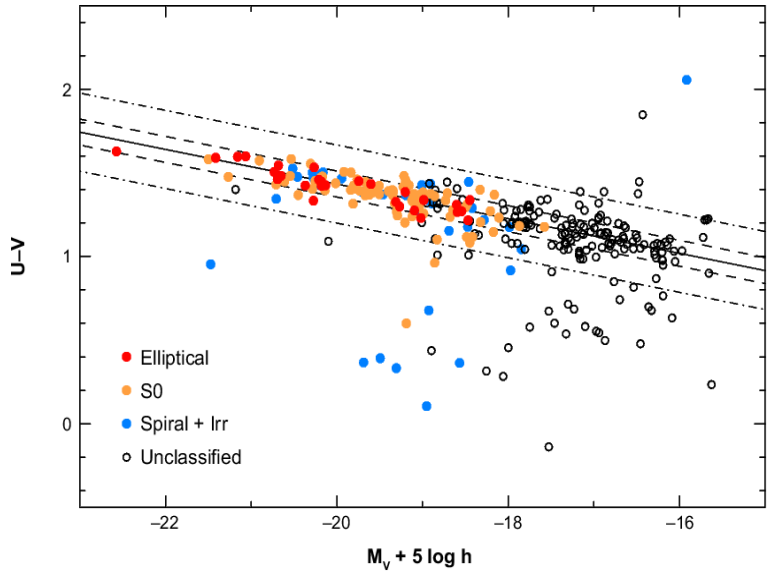


Figure 3: The $(U-V)-M_{\rm V}$ color-magnitude relation for galaxies of the various morphological types that are spectroscopic members of the Coma cluster (Bower et al. 1999).

The C-M relation looked the same in all nine studied clusters, and much the same in the field as well, though with larger dispersion (at least in part due to larger distance errors). The focus was on the possible use of the C-M relation as a distance indicator; however, Sandage & Visvanathan documented the tightness of the relation and noted that it implies the stellar content of the galaxies to be very uniform. They also estimated that both S0's and ellipticals had to be evolving passively since at least $\sim 1$ Gyr ago. Figure 3 shows a modern rendition for the C-M plot for the Coma cluster galaxies, showing how tight it is, as well as how closely both S0's and ellipticals follow the same relation, as indeed Sandage & Visvanathan had anticipated.

In a major breakthrough in galaxy dating, Bower, Lucey, & Ellis (1992), rather than trying to age-date galaxies one by one, were able to set tight age constraints on all ETGs in Virgo and Coma at once. Noting the remarkable homogeneity of ETGs in these clusters, they estimated the intrinsic color scatter in the color-$\sigma$ relation (see Figure 4) to be $\delta(U-V)\lesssim 0.04$ mag, where $\sigma$ is the central stellar velocity dispersion of these galaxies. They further argued that – if due entirely to an age dispersion $\delta t = \beta(t_{\rm H}-t_{\rm F})$, such color scatter should be equal to the time scatter in formation epochs, times $\partial(U-V)/\partial t$, i.e.:

$$t_{\rm H}-t_{\rm F} \lesssim \frac{0.04}{\beta}\Big(\frac{\partial(U-V)}{\partial t}\Big)^{-1}, \qquad (1)$$

where $t_{\rm H}$ is the age of the universe at $z=0$, and galaxies are assumed to form before a lookback time $t_{\rm F}$. Bower and colleagues introduced the parameter $\beta$, such that $\beta(t_{\rm H}-t_{\rm F})$ is the fraction of the available time during which galaxies actually form. Thus, for $\beta=1$ galaxy formation is uniformly distributed between $t\sim 0$ and $t=t_{\rm H}-t_{\rm F}$ , whereas for $\beta<1$ it is more and more synchronized, i.e., restricted to the fraction $\beta$ of time interval $t_{\rm H}-t_{\rm F}$. Adopting $\partial(U-V)/\partial t$ from the models of Bruzual (1983), they derived $t_{\rm H}-t_{\rm F}<2$ Gyr for $\beta=1$ and $t_{\rm H}-t_{\rm F}<8$ Gyr for $\beta=0.1$, corresponding respectively to formation redshifts

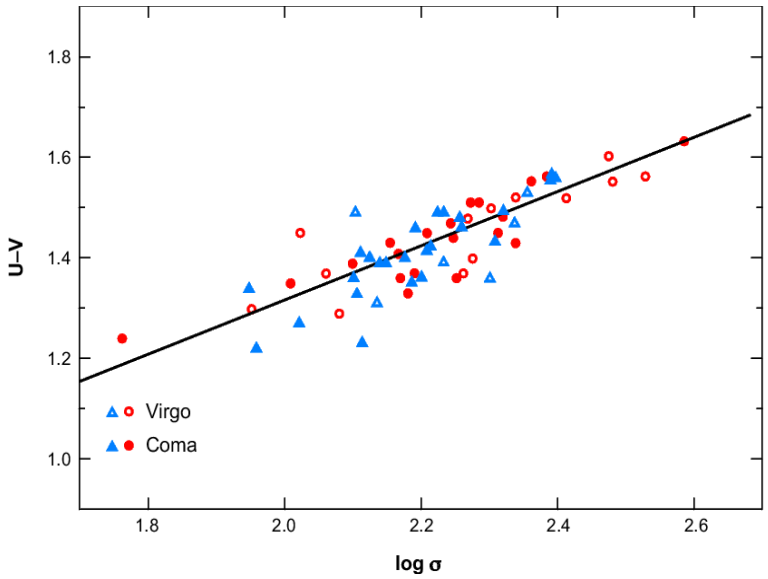


Figure 4: The relation between the $(U-V)$ color and the central velocity dispersion ($\sigma$) for early-type galaxies in the Virgo (open symbols) and Coma (filled symbols) clusters. Red circles represent ellipticals, blue triangles represent S0's. From Bower, Lucey & Ellis (1992).

$z_{\rm F}\gtrsim 2.8$ and $\gtrsim 1.1$ for their adopted cosmology ($t_{\rm H}=15$ Gyr, $q_\circ=0.5$). For the concordance cosmology, the same age constraints imply $z_{\rm F}\gtrsim 3.3$ and $\gtrsim 0.8$, respectively. A value $\beta=0.1$ implies an extreme synchronization, with all Virgo and Coma galaxies forming their stars within less than 1 Gyr when the universe had half its present age, which seems rather implausible. Bower and colleagues concluded that ellipticals in clusters formed the bulk of their stars at $z\gtrsim 2$, and later additions should not provide more than $\sim 10\%$ of their present luminosity. Making minimal use of stellar population models, this approach provided for the first time a robust demonstration that cluster ellipticals are made of very old stars, with the bulk of them having formed at $z\gtrsim 2$.

As the narrowness of the C-M and color-$\sigma$ relations sets constraints on the ages of stellar populations in ETGs, their slope can set useful constraints on the amount of merging that may have led to the present-day galaxies. The reason is that merging without star formation increases luminosity and $\sigma$, but leaves colors unchanged, thus broadening and flattening the relations. Moreover, merging with star formation makes bluer galaxies, thus broadening and flattening the relations even more. Then, from the constraints set by the slope of the C-M relation, Bower, Kodama, & Terlevich (1998) concluded that not only the bulk of stars in clusters must have formed at high redshift, but also that they cannot have formed in mass units much less than about half their present mass.

3.1.2 THE FUNDAMENTAL PLANE Three key observables of elliptical galaxies, namely the effective radius $R_{\rm e}$, the central velocity dispersion $\sigma$, and the luminosity $L$ (or equivalently the effective surface brightness $I_{\rm e}=L/2\pi {R_{\rm e}}^2$) relate their structural/dynamical status to their stellar content. Indeed, elliptical galaxies are not randomly distributed within the 3D space $(R_{\rm e},\sigma,I_{\rm e})$, but rather cluster close to a plane, thus known as the fundamental plane (FP), with $R_{\rm e}\propto \sigma^{\rm a} {I_{\rm e}}^{\rm b}$ (Dressler et al. 1987; Djorgovski & Davis 1987), where the exponents $a$ and $b$ depend on the specific band used for measuring the luminosity. The projection of

the FP over the $(R_{\rm e}, I_{\rm e})$ coordinate plane generates the Kormendy relation (Kormendy 1977), whereas a projection over the $(\sigma, L = 2\pi {R_{\rm e}}^2 I_{\rm e})$ plane generates the Faber-Jackson relation (Faber & Jackson 1976). At a time when testing the $\Omega_{\rm M} = 1$ standard cosmology had high priority, the FP was first used to estimate distances, in order to map deviations from the local Hubble flow and construct the gravitational potential on large scales. Its use to infer the properties of the stellar content of galaxies, and set constraints on their formation, came later. Yet, by relating the luminosity to the structural-dynamical parameters of a galaxy, the FP offers a precious tool to gather information on the ages and metallicities of galaxies, at low as well as at high redshifts.

The mere existence of a FP implies that ellipticals (*a*) are virialised systems, (*b*) have self-similar (homologous) structures, or their structures (e.g., the shape of the mass distribution) vary in a systematic fashion along the plane, and (*c*) contain stellar populations which must fulfill tight age and metallicity constraints. Here we concentrate on this latter aspect.

To better appreciate the physical implications of the FP, Bender, Burnstein, & Faber (1992) introduced an orthogonal coordinate system $(\kappa_1, \kappa_2, \kappa_3)$, in which each new variable is a linear combination of $\log \sigma^2$, $\log R_{\rm e}$ and $\log I_{\rm e}$. The transformation corresponds to a rotation of the coordinate system such that in the $(\kappa_1, \kappa_3)$ projection the FP is seen almost perfectly edge-on. Moreover, if structural homology holds all along the plane, then $\log M/L = \sqrt{3}\kappa_3 + \text{const}$. If $\sigma$ is (almost) unaffected by the dark matter distribution (as currently understood, Rix et al. 1997), then $\kappa_3$ provides a measure of the stellar $M/L$ ratio, and $\kappa_1 \propto \log(\sigma^2 R_{\rm e}) \propto \log M$ a measure of the stellar mass. Bender and colleagues showed that in Virgo and Coma the FP is remarkably "thin", with a 1-$\sigma$ dispersion perpendicular to the plane of only $\sigma(\kappa_3) \simeq 0.05$, corresponding to a dispersion in the $M/L$ ratio $\lesssim$10% at any position along the plane. Moreover, the FP itself is "tilted", with the $M/L$ ratio apparently increasing by a factor $\sim 3$ along the plane, while the mass is increasing by a factor $\sim 100$. Note that the tilt does not imply a departure from virialization, but rather a systematic trend of the stellar content with galaxy mass, possibly coupled with a systematic departure from structural homology (e.g., Bender, Burstein & Faber 1992, Ciotti 1997, Busarello et al. 1997).

The narrowness of the FP, coupled to the relatively large tilt ($\Delta\kappa_3/\sigma(\kappa_3) \simeq 0.35/0.05 = 7$) requires some sort of fine tuning, which is perhaps the most intriguing property of the FP (Renzini & Ciotti 1993). Although unable to identify one specific origin for the FP tilt, Renzini & Ciotti argued that the small scatter perpendicular to the FP implied a small age dispersion ($\lesssim$15%) and high formation redshift, fully consistent with the Bower, Lucey & Ellis (1992) argument based on the narrowness of the C-M and color-$\sigma$ relations.

The remarkable properties of the FP for the Virgo and Coma clusters were soon shown to be shared by all studied clusters in the local universe. Jørgensen, Franx, & Kjærgaard (1996) constructed the FP for 230 ETGs in 10 clusters (including Coma), showing that the FP tilt and scatter are just about the same in all local clusters, thus strengthening the case for the high formation redshift of cluster ETGs being universal. However, Worthey, Trager, & Faber (1995) countered that the thinness of the FP, C-M, and color-$\sigma$ relations could be preserved, even with a large age spread, provided age and metallicity are anticorrelated (with old galaxies being metal poor and young ones being metal rich). This is indeed what Worthey and colleagues reported from their line-indices analysis (see below),

indicating a factor of $\sim 6$ for the range in age balanced by a factor $\sim 10$ in metallicity (from solar to $\sim 10$ times solar). If so, then the FP should be thicker in the near infrared, because the compensating effect of metallicity would be much lower at longer wavelength, thus unmasking the full effect of a large age spread (Pahre, Djorgovski, & De Carvalho 1995). But Pahre and colleagues found the scatter of the FP $K$-band to be the same as in the optical. In addition, its slope implied a sizable variation of $M/L_{\rm K} \propto M^{0.16}$ along the FP, somewhat flatter than in the optical ($M/L_{\rm V} \propto M^{0.23}$), still far from the $M/L_{\rm K}$ ∼const. predicted by Worthey et al. (1995).

These conclusions were further documented and reinforced by Pahre, Djorgovski, & De Carvalho (1998), Scodeggio et al. (1998), Mobasher et al. (1999), and Pahre, De Carvalho, & Djorgovski (1998), who finally concluded that the origin of the FP tilt defies a simple explanation, but is likely the result of combined age and metallicity trends along the plane (with the most metal rich galaxies being actually the oldest), plus an unidentified systematic deviation from structural homology. Several possibilities for the homology breaking have been proposed and investigated, such as variation in stellar and/or dark matter content and/or distribution, anisotropy, and rotational support (e.g., Ciotti, Lanzoni, & Renzini 1996, Prugniel & Simien 1996, Ciotti & Lanzoni 1997). Recently, Trujillo, Burkert, & Bell (2004) argued that one fourth of the tilt is due to stellar population (i.e., a combination of metallicity and age), and three quarters of it to structural nonhomology in the distribution of the visible matter.

Of special interest is the comparison of the FP in clusters and in the field, because one expects all formation processes to be faster in high density peaks of the matter distribution. This was tested by Bernardi et al. (2003b, 2006) with a sample of $\sim 40,000$ SDSS morphology- and color-selected ETGs spanning a wide range of environmental conditions, from dense cluster cores to very low densities. Bernardi and colleagues found very small, but detectable differences in the FP zero point; the average surface brightness is $\sim 0.08$ mag brighter at the lowest density extreme compared to the opposite extreme. As the sample galaxies are distributed in redshift up to $z \sim 0.3$, they used the observed lookback time to empirically determine the time derivative of the surface brightness (hence in a model-independent fashion) and estimated that the 0.08 mag difference in surface brightness implies an age difference of $\sim 1$ Gyr, and therefore that galaxies in low density environments are $\sim 1$ Gyr younger compared to those in cluster cores.

3.1.3 THE LINE-STRENGTH DIAGNOSTICS Optical spectra of ETGs present a number of absorption features whose strength must depend on the distributions of stellar ages, metallicities and abundance ratios, and therefore may give insight over such distributions. To exploit this opportunity, Burstein et al. (1984) introduced a set of indices now known as the Lick/IDS system, and started taking measurements for a number of galaxies. The most widely used indices have been the $\rm Mg_2$ (or Mg$b$), $<$Fe$>$, and the H$\beta$ indices, measuring respectively the strength of MgH+MgI at $\lambda \simeq 5156 - 5197$Å, the average of two FeI lines at $\lambda \simeq 5248$ and 5315Å, and of $\rm H_\beta$.

A first important result was the discovery that theoretical models based on solar abundance ratios adequately describe the combinations of the values of the $<$Fe$>$ and $\rm Mg_2$ indices in low-luminosity ETGs, but fail for bright galaxies (Peletier 1989, Gorgas, Efstathiou, & Aragón-Salamanca 1990, Faber, Worthey, & Gonzales 1992, Worthey, Faber, & Gonzales 1992, Davies, Sadler, & Peletier

1993, Jørgensen 1997). This implies either that population synthesis models suffered from some inadequacy at high metallicity (possibly due to incomplete stellar libraries), or that massive ellipticals were genuinely enriched in magnesium relative to iron, not unlike the halo stars of the Milky Way (e.g., Wheeler, Sneden, & Truran 1989). As for the Milky Way halo, such an $\alpha$-element overabundance may signal a prompt enrichment in heavy elements from Type II supernovae, with the short star-formation timescale having prevented most Type Ia supernovae from contributing their iron while star formation was still active. Yet, a star-formation timescale decreasing with increasing mass was contrary to the expectations of galactic wind/monolithic models (e.g., Arimoto & Yoshii 1987), where the star formation timescale increases with the depth of the potential well (Faber, Worthey & Gonzales 1992). However, as noted by Thomas (1999), the contemporary semi-analytical models did not predict any $\alpha$-element enhancement at all, no matter whether in low- or high-mass ETGs. Indeed, Thomas, Greggio, & Bender (1999) argued that the $\alpha$-enhancement, if real, was also at variance with a scenario in which massive ellipticals form by merging spirals, and required instead that star formation was completed in less than $\sim 1$ Gyr. Therefore, assessing whether the $\alpha$-enhancement was real, and in that case measuring it, had potentially far reaching implications for the formation of ETGs.

Two limitations had to be overcome in order to reach a credible interpretation of the $<\mathrm{Fe}> - \mathrm{Mg}b$ plots: (*a*) existing synthetic models for the Lick/IDS indices were based on stellar libraries with fixed [$\alpha$/Fe] (Worthey 1994, Buzzoni 1995), and (*b*) an empirical verification of the reality of the $\alpha$-enhancement was lacking. In an attempt to overcome the first limitation, Greggio (1997) developed a scaling algorithm that allowed one to use existing models with solar abundance ratios to estimate the Mg overabundance, and she concluded that an enhancement up to [Mg/Fe]$\simeq +0.4$ was required for the nuclei of the most massive ellipticals (see also Weiss, Peletier, & Matteucci 1995). She also concluded that a closed-box model for chemical evolution failed to explain the very high values of the $\mathrm{Mg}_2$ index of these galaxies. Indeed, the numerous metal-poor stars predicted by the model would obliterate the $\mathrm{Mg}_2$ feature, hence the nuclei of ellipticals had to lack substantial numbers of stars more metal poor than $\sim 0.5 Z_{\odot}$. Besides, very old ages ($\gtrsim$10 Gyr) and $\alpha$-enhancement were jointly required to account for galaxies with strong $\mathrm{Mg}_2$. Eventually, Thomas, Maraston, & Bender (2003) produced a full set of synthetic models with variable [$\alpha$/Fe], and Maraston et al. (2003) compared such models to the indices of ETGs and of metal-rich globular clusters of the Galactic bulge, for which the $\alpha$-enhancement has been demonstarted on a star-by-star basis by high resolution spectroscopy. The result is displayed in Figure 5, showing that indeed the new models indicate for the bulge globulars an enhancement of [$\alpha$/Fe]$\sim +0.3$, in agreement with the stellar spectroscopy results, and similar to that indicated for massive ETGs.

Other widely used diagnostic diagrams involved the H$\beta$ index along with $<\mathrm{Fe}>$ and $\mathrm{Mg}_2$ or Mg*b*. The Balmer lines had been suggested as good age indicators (e.g., O'Connell 1980; Dressler & Gunn 1983), an expectation that was confirmed by the set of synthetic models constructed by Worthey (1994) with the aim of breaking the age-metallicity degeneracy that affects the broad-band colors of galaxies. Worthey's models were applied by Jørgensen (1999) to a sample of 115 ETGs in the Coma cluster, and by Trager et al. (2000) to a sample of 40 ETGs biased toward low-density environments, augmented by 22 ETGs in the Fornax cluster from Kuntschner & Davies (1998), which showed systematically lower H$\beta$

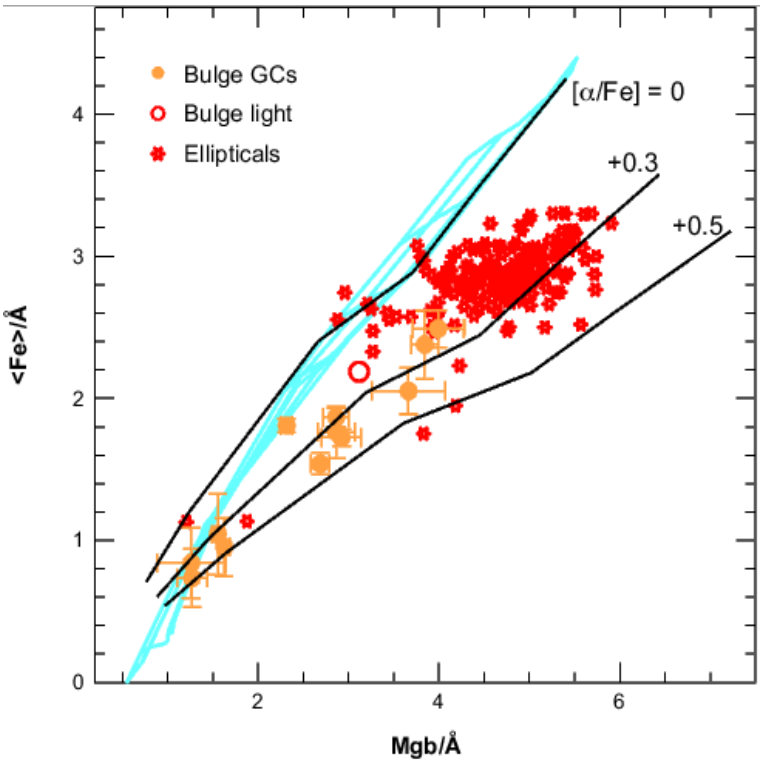


Figure 5: The $<$Fe$>$ index versus the Mg$b$ index for a sample of halo and bulge globular clusters, the bulge integrated light in Baade's Window, and for elliptical galaxies from various sources. Overimposed are synthetic model indices (from Thomas, Maraston & Bender 2003) with solar metallicity ([Z/H]=0), various $\alpha$-enhancements as indicated, and an age of 12 Gyr (black solid lines). The cyan grid shows a set of simple stellar population models (from Maraston 1998) with solar abundance ratios, metallicities from [Fe/H] = –2.25 to +0.67 (bottom to top), and ages from 3 to 15 Gyr (left to right). The blue grid offers an example of the so-called age-metallicity degeneracy. From Maraston et al. (2003).

indices. From these samples, and using the H$\beta$ – Mg$b$ and H$\beta$ – $<$Fe$>$ plots from Worthey's models, both Jørgensen and Trager and colleagues concluded that ages ranged from a few to almost 20 Gyr, but age and metallicity were anticorrelated in such a way that the Mg$b$ – $\sigma$, C-M, and FP relations may be kept very tight. Moreover, there was a tendency for ETGs in the field to appear younger than those in clusters. Yet, Trager and colleagues cautioned that H$\beta$ is most sensitive to even low levels of recent star formation, and suggested that the bulk of stars in ETGs may well be old, but a small "frosting" of younger stars drives some galaxies toward areas in the H$\beta$ – Mg$b$ and H$\beta$ – $<$Fe$>$ plots with younger SSP ages. Finally, for the origin of the $\alpha$-enhancement Trager and colleagues favored a tight correlation of the IMF with $\sigma$, in the sense of more massive galaxies having a flatter IMF, hence more Type II supernovae. However, with a flatter IMF more massive galaxies would evolve faster in luminosity with increasing redshift, compared to less massive galaxies, which appears to be at variance with the observations (see below).

These conclusions had the merit of promoting further debates. Maraston & Thomas (2000) argued that even a small old, metal-poor component with a blue horizontal branch (like in galactic globulars) would increase the H$\beta$ index thus

making galaxies look significantly younger than they are. Even more embarrassing for the use of the H$\beta$ − Mg$b$ and H$\beta$ − $<$Fe$>$ plots is that a perverse circulation of the errors automatically generates an apparent anticorrelation of age and metallicity, even where it does not exist. For example, if H$\beta$ is overestimated by observational errors, then age is underestimated, which in turn would reduce Mg$b$ below the observed value unless the younger age is balanced by an artificial increase of metallicity. Trager and colleagues were fully aware of the problem, and concluded that only data with very small errors could safely be used. Kuntschner et al. (2001) investigated the effect by means of Monte Carlo simulations, and indeed showed that much of the apparent age-metallicity anticorrelation is a mere result of the tight correlation of their errors. They concluded that only a few outliers among the 72 ETGs in their study are likely to have few-billion-year-old luminosity-weighted ages, and these were typically galaxies in the field or loose groups, whereas a uniformly old age was derived for the vast majority of the studied galaxies. Moreover, younger ages were more frequently indicated for S0 galaxies (Kuntschner & Davies 1998). Nevertheless, in a cluster with very tight C-M and FP relations such as Coma, a large age spread at all magnitudes was found for a sample of 247 cluster members (Poggianti et al. 2001), and a sizable age-metallicity anticorrelation was also found for a large sample of SDSS galaxies (Bernardi et al. 2005).

As already alluded to, the main pitfall of the procedure is that the various indices depend on all three population parameters one is seeking to estimate: thus H$\beta$ is primarily sensitive to age, but also to [Fe/H] and [$\alpha$/Fe], $<$Fe$>$ is sensitive to [Fe/H], but also to age and [Mg/Fe]; etc. Thus, the resulting errors in age, [Fe/H] and [Mg/Fe] are all tightly correlated, and one is left with the suspicion that apparent correlations or anticorrelations may be an artifact of the procedure, rather than reflecting the real properties of galaxies. In an effort to circumvent these difficulties, Thomas et al. (2005) renounced to trust the results galaxy by galaxy. They rather looked at patterns in the various index-index plots and compared them to mock galaxy samples generated via Monte Carlo simulations that fully incorporated the circulation of the errors. The real result was not a set of ages and metallicities assigned to individual galaxies, but rather age and metallicity trends with velocity dispersion, mass and environments. Having analyzed a sample of 124 ETGs in high- and low-density environments, Thomas and colleagues reached the following conclusions: ($a$) all three parameters –age, metallicity and [$\alpha$/Fe]– correlate strongly with $\sigma$, and, on average, follow the relations:

$$\log t/\mathrm{Gyr} = 0.46\,(0.17) + 0.238\,(0.32)\log\,\sigma, \tag{2}$$

$$[\mathrm{Z/H}] = -1.06\,(-1.03) + 0.55\,(0.57)\log\,\sigma, \tag{3}$$

$$[\alpha/\mathrm{Fe}] = -0.42\,(-0.42) + 0.28\,(0.28)\log\,\sigma, \tag{4}$$

where quantities in brackets/not in brackets refer to low-density/high-density environments, respectively. ($b$) For ETGs less massive than $\sim 10^{10} M_{\odot}$ there is evidence for the presence of intermediate-age stellar populations with near-solar Mg/Fe. Instead, massive galaxies ($\gtrsim 10^{11} M_{\odot}$) appear dominated by old stellar populations, whereas at intermediate masses the strength of H$\beta$ requires either some intermediate age component or a blue horizontal branch (HB) contribution. ($c$) By and large this picture applies to both cluster and field ETGs, with cluster galaxies having experienced the bulk of their star formation between $z \sim 5$ and 2, and this activity appears to have been delayed by $\sim 2$ Gyr in the lowest density

environments, i.e., between $z \sim 2$ and $\sim 1$. Figure 6 qualitatively summarizes this scenario, in which the duration of star formation activity decreases with increasing mass (as required by the [Mg/Fe] trend with $\sigma$), and extends to younger ages for decreasing mass (as forced by the $H\beta - \sigma$ relation). Note that the smooth star-formation histories in this figure should be regarded as probability distributions, rather than as the actual history of individual galaxies, where star formation may indeed take place in a series of bursts. Qualitatively similar conclusions were reached by Nelan et al. (2005), from a study of $\sim 4000$ red-sequence galaxies in $\sim 90$ clusters as part of the National Astronomical Observatory Fundamental Plane Survey. Assuming the most massive galaxies ($\sigma \sim 400\,\mathrm{km\ s^{-1}}$) to be 13 Gyr old, they derived an age of only 5.5 Gyr for less massive galaxies ($\sigma \sim 100\,\mathrm{km\ s^{-1}}$). Note that the age-$\sigma$ scaling of Thomas and colleagues would have given a much older age ($\sim 9.5$ Gyr). Taken together, Equations 2 and 3 imply a trend of $M/L_V$ by a factor $\sim 1.8$ along the FP (from $\sigma = 100$ to 350 km s$^{-1}$), thus accounting for almost two thirds of the FP tilt.

As extensively discussed by Thomas et al. (2005), one residual concern comes from the possibility that part of the H$\beta$ strength may be due to blue HB stars. Besides a blue HB contribution by low-metallicity stars (especially in less massive galaxies), blue HB stars may also be produced by old, metal-rich populations, and appear to be responsible for the UV upturn in the spectrum of local ETGs (Brown et al. 2000, Greggio & Renzini 1990). In the Thomas et al. sample, some S0 outliers with strong H$\beta$ and strong metal lines would require very young ages and extremely high metallicity (up to $\sim 10$ times solar), and may better be accounted for by an old, metal-rich population with a well-developed blue HB.

The $Mg_2 - \sigma$ relation has also been used to quantify environmental differences in the stellar population content. The cluster/field difference turns out to be small, with $\Delta Mg_2 \sim 0.007$ mag, corresponding to $\sim 1$ Gyr difference – field galaxies being younger – within a sample including $\sim 900$ ETGs (Bernardi et al. 1998), though no statistically significant environmental dependence of both $Mg_2$ and H$\beta$ was detected within a sample of $\sim 9,000$ ETGs from the SDSS (Bernardi et al. 2003a). Still from SDSS, coadding thousands of ETG spectra in various luminosity and environment bins, Eisenstein et al. (2003) detect clear trends with the environment thanks to the resulting exquisite S/N, but the differences are very small, and Eisenstein and colleagues refrain from interpreting them in terms of age/metallicity differences.

These results from the analysis of the Lick/IDS indices, including large trends of age with $\sigma$, or even large age-metallicity anticorrelations, have yet to be proven consistent with the FP and C-M relations of the same galaxies as established specifically for the studied clusters. Feeding the values of the indices, the synthetic models return ages, metallicities, and $\alpha$-enhancements. But along with them the same models also give the colors and the stellar $M/L$ ratio of each galaxy in the various bands, hence allowing one to construct implied FP and C-M relations. It would be reassuring for the soundness of the whole procedure if such relations were found to be consistent with the observed ones. To our knowledge, this sanity check has not been attempted yet. The mentioned trends and correlations, if real, would also have profound implications for the evolution of the FP and C-M relations with redshift, an opportunity that will be exploited below.

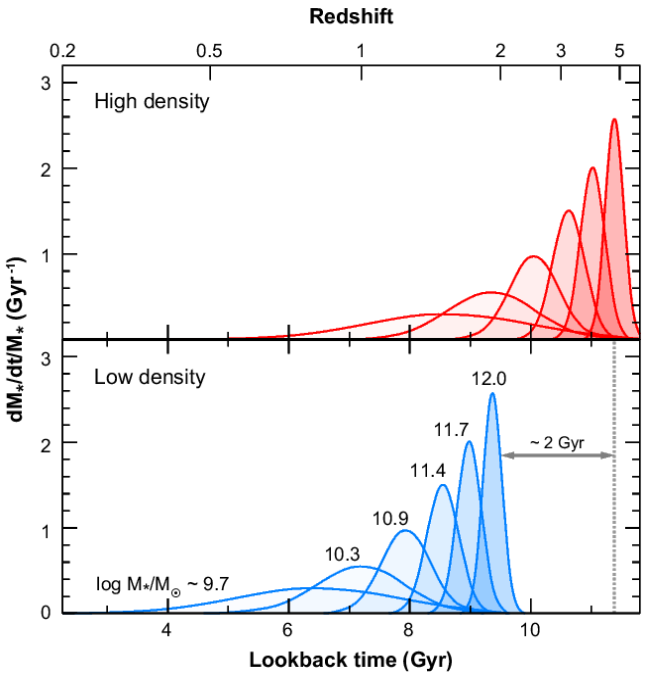


Figure 6: The scenario proposed by Thomas et al. (2005) for the average star formation history of early-type galaxies of different masses, from $5 \times 10^9 M_\odot$ up to $10^{12} M_\odot$, corresponding to $\sigma \simeq 100$ to $\sim 320$ km s$^{-1}$, for the highest and lowest environmental densities, respectively, in the upper and lower panel.

### *3.2 Ellipticals Versus Spiral Bulges*

The bulges of spiral galaxies are distinguished in "true bulges", typically hosted by S0-Sb galaxies, and "pseudobulges" usually (but not exclusively) in later-type galaxies (Kormendy & Kennicutt 2004). True (classical) bulges have long been known as similar to ellipticals of comparable luminosity, in both structure, line strengths and colors (e.g., Bender, Burnstein & Faber 1992, Jablonka, Martin, & Arimoto 1996, Renzini 1999, and references therein). Peletier et al. (1999) were able to quantify this similarity using *Hubble Space Telescope* (HST) WFPC2 (Wide Field Planetary Camera 2) and NICMOS (Near Infrared Camera and Multiobject Spectrometer) observations, and concluded that most (true) bulges in their sample of 20 spirals (including only 3 galaxies later than Sb) had optical and optical-IR colors similar to those of Coma ellipticals. Hence, like in Coma ellipticals their stellar populations formed at $z \gtrsim 3$, even if most of the galaxies in their sample are in small groups or in the field. More recently, Falcon-Barroso, Peletier, & Balcells (2002) measured the central velocity dispersion for the same sample observed by Peletier and colleagues, and constructed the FP for these bulges, showing that bulges in this sample tightly follow the same FP relation as cluster ellipticals, and therefore had to form their stars at nearly the same epoch. The similarity of true bulges and ellipticals includes the tendency of less massive objects to have experienced recent star formation, as indicated by their location in the $\mathrm{Mg}_2 - \sigma$ diagram in Figure 7. These similarities between true (classical) bulges and ellipticals suggest a similar origin, possibly in merger-driven starbursts at high redshifts. Pseudobulges, instead, are more likely to

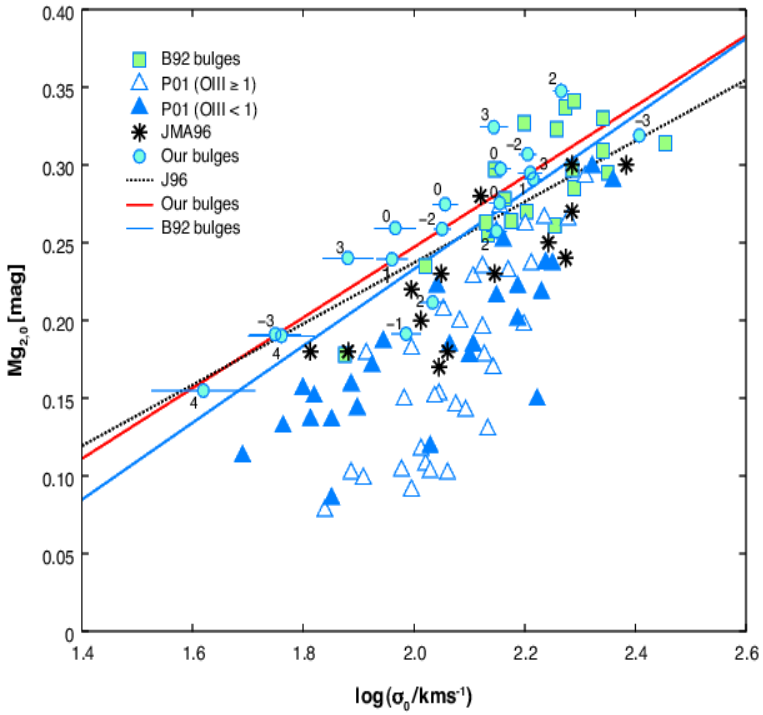


Figure 7: The $Mg_2 - \sigma$ relation for the spiral bulges studied by Falcon-Barroso et al. (2002), labelled "our bulges" in the insert, are compared to bulges in other samples (B92 = Bender, Burnstein & Faber 1992, P01 = Prugniel, Maubon & Simien 2001, JMA96 = Jablonka, Martin & Arimoto 1996). The solid lines are the bet fits to the corresponding data, while the dashed line show the average relation for cluster ellipticals from Jørgensen, Franx & Kjærgaard (1996).

have originated via secular evolution of disks driven by bars and other deviations from axial symmetry, as extensively discussed and documented by Kormendy & Kennicutt (2004). Several of the objects in the Prugniel and colleagues sample in Figure 7 are likely to belong to the pseudobulge group. From the Lick/IDS indices of a sample of bulges, Thomas and Davies (2006) argue that the same scenario depicted in Figure 6 for ETGs, applies to bulges as well, the main difference being that bulges are on average less massive, hence on average younger than ETGs.

Looking near to us, HST and ground based photometry of individual stars in the Galactic bulge have shown that they are older than at least 10 Gyr, with no detectable trace of an intermediate age component (Ortolani et al. 1995, Kuijken & Rich 2002, Zoccali et al. 2003). HST/NICMOS photometry of stars in the bulge of M31 has also shown that their $H$-band luminosity function is virtually identical to that of the Galactic bulge, and by inference should have nearly identical ages (Stephens et al. 2003). These two bulges belong to spirals in a rather small group, and yet appear to have formed their stars at an epoch corresponding to $z \gtrsim 2$, not unlike most ellipticals.

### *3.3 Summary of the Low-Redshift (Fossil) Evidence*

The main observational constraints on the epoch of formation of the stellar populations of ETGs in the near universe can be summarized as follows:

- The C-M, color-$\sigma$ and FP relations for ETGs in clusters indicate that the

bulk of stars in these galaxies formed at $z \gtrsim 2-3$.

- The same relations for the field ETGs suggest that star formation in low density environments was delayed by $\sim 1-2$ Gyr.
- The more massive galaxies appear to be enhanced in Mg relative to iron, which indicates that the duration of the star-formation phase decreases with increasing galaxy mass, having been shorter than $\sim 1$ Gyr in the most massive galaxies.
- Interpretations of the Lick/IDS indices remains partly controversial, with either an age-metallicity anticorrelation, or an increase of both age and metallicity with increasing $\sigma$.

These trends are qualitatively illustrated in Figure 6, showing that the higher the final mass of the system, the sooner star formation starts and more promptly subsides, in an apparently "antihierarchical" fashion. A trend in which the stellar population age and metallicity are tightly correlated to the depth of the potential well (as measured by $\sigma$) argues for star formation, metal enrichment, supernova feedback, merging, and violent relaxation having been all concomitant processes rather than having taken place sequentially.

The fossil evidence illustrated so far is in qualitative agreement with complementary evidence at low as well as high redshift, now relative to star-forming galaxies as opposed to quiescent ones. At low $z$, Gavazzi (1993) and Gavazzi, Pierini, & Boselli (1996) showed that in local (disk) galaxies the specific star-formation rate anticorrelates with galaxy mass, a trend that can well be extended to include fully quiescent ellipticals. On this basis, Gavazzi and collaborators emphasized that mass is the primary parameter controlling the star-formation history of galaxies, with a sharp transition at $L_{\rm H} \simeq 2\times10^{10}L_{\odot}$ (corresponding to $\sim 2\times10^{10}M_{\odot}$) between late-type, star-forming galaxies and mostly passive, early-type galaxies (Scodeggio et al. 2002). This transition mass has then been precisely located at $\sim 3\times10^{10}M_{\odot}$ with the thorough analysis of the SDSS database (Kauffmann et al. 2003). In parallel, high redshift observations have shown that the near-IR luminosity (i.e., mass) of galaxies undergoing rapid star formation has declined monotonically from $z \sim 1$ to the present, a trend for which Cowie et al. (1996) coined the term down-sizing. This is becoming a new paradigm for galaxy formation, as the anticorrelation of the specific star-formation rate with mass is now recognized to persist well beyond $z \sim 2$ (e.g., Juneau et al. 2005, Feulner et al. 2006).

## 4 ELLIPTICAL GALAXIES AT HIGH REDSHIFT

Perhaps the best way of breaking the age-metallicity degeneracy is by looking back in time, studying galaxies at higher and higher redshifts. In the 1990s this was attempted first with 4m-class telescopes, and later, with impressive success, with 8-10m-class telescopes and HST. Studies first focused on cluster ellipticals, and their extension to field galaxies followed with some delay. Thus, the evolution with redshift of various galaxy properties were thoroughly investigated, such as the C-M and Kormendy relations, the luminosity and mass functions, and the FP. Various ongoing surveys are designed to map the evolution with redshift and local environment of all these properties, along with the number density of these galaxies.

### *4.1 Cluster Ellipticals Up to $z \sim 1$*

4.1.1 THE COLOR-MAGNITUDE RELATION With the identification of clusters at higher and higher redshifts, from the mid-1990s it became possible to construct their C-M relation, hence to directly assess the rate of evolution of cluster ETGs. Pioneering studies showed a clearly recognizable red sequence in high-redshift clusters, and gave hints that the color evolution up to $z \sim 1$ was broadly consistent with pure passive evolution of the galaxies formed at high redshift (Dressler & Gunn 1990; Aragón-Salamanca et al. 1993; Rakos & Schombert 1995). Subsequent studies fully confirmed these early hints and provided accurate estimates for the formation redshift of the bulk of stars in cluster ellipticals. Thus, replicating the Bower, Lucey & Ellis (1992) procedure for a sample of morphologically-selected ETGs in clusters at $z \sim 0.5$, Ellis et al. (1997) were able to conclude that most of the star formation in ellipticals in dense clusters was completed 5–6 Gyr earlier than the cosmic time at which they are observed, i.e., at $z \gtrsim 3$. Extending these studies to clusters up to $z \sim 0.9$, Stanford, Eisenhardt, and Dickinson (1998) showed that pure passive evolution continues all the way to such higher redshift, while the dispersion of the C-M relation remains as small as it is in Virgo and Coma (see Figure 8). Thus, Stanford and colleagues concluded that cluster ellipticals formed the bulk of their stars at $z \gtrsim 3$, with the small color dispersion arguing for highly synchronized star-formation histories among galaxies within each cluster, and from one cluster to another. These conclusions were reinforced by several other investigators, e.g., Gladders et al. (1998), Kodama et al. (1998), Nelson et al. (2001), De Lucia et al. (2004), and by van Dokkum et al. (2000), who also cautioned about the "progenitor bias" (see below).

The evolution of the C-M relation was then traced beyond $z = 1$ thanks to the discovery of higher redshift clusters, primarily by the Rosat Deep Cluster Survey (RDCS, Rosati et al. 1998). Using deep HST/ACS (Advanced Camera for Surveys) $i$- and $z$-band images, Blakeslee et al. (2003) found a tight red sequence for morphologically selected ETGs in a $z = 1.24$ cluster, implying typical ages of $\sim 3$ Gyr, and formation redshift $z_{\rm F} \gtrsim 3$. This was further confirmed by its infrared C-M relation (Lidman et al. 2004). However, some clusters in the range $0.78 < z < 1.27$ appear to have a larger color scatter than others, again with ellipticals in those with tight C-M relation having virtually completed their star formation at $z \gtrsim 3$ (Holden et al. 2004). Presently, the highest redshift clusters known to be dominated by old, massive ETGs are at $z \simeq 1.4$ (Stanford et al. 2005, Mullis et al. 2005).

The redshift evolution of the color of the red sequence in clusters proved to be a very powerful tool in disentangling ambiguities that are difficult to eliminate based only on $z \sim 0$ observations. From the color evolution of the red sequence in two Abell clusters at $z \sim 0.2$ and $\sim 0.4$, Kodama & Arimoto (1997) were able to break the age-metallicity degeneracy plaguing most of the global observables of local ellipticals. In principle, because colors depend both on age and metallicity, the slope of the C-M relation could equally well be reproduced with either age or metallicity increasing with increasing luminosity (or $\sigma$). However, if age were the dominant effect, then the C-M relation would steepen with lookback time (redshift), as the color of the young galaxies would get more rapidly bluer compared to that of the old galaxies. Instead, the slope of the relation remains nearly the same (see Figure 8). Actually, the Kodama & Arimoto argument can be applied

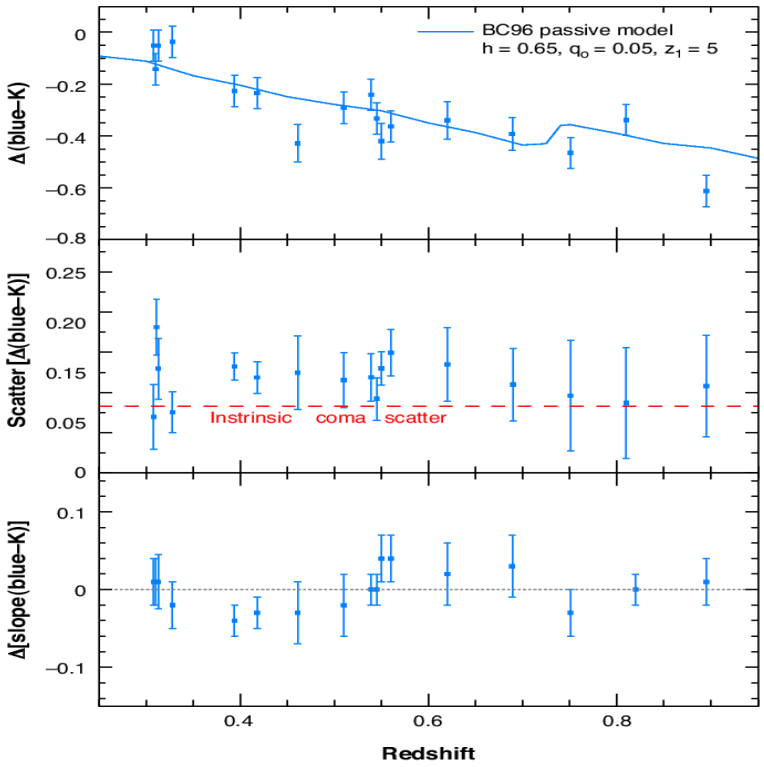


Figure 8: The color evolution of early-type galaxies in clusters out to $z \simeq 0.9$ (Stanford, Eisenhardt & Dickinson 1998, Dickinson 1997). The "blue" band is tuned for each cluster to approximately sample the rest frame $U$-band, whereas the $K$ band is always in the observed frame. Top panel: the redshift evolution of the zero point of "blue"$-K$ color-magnitude (C-M) relation relative to the Coma cluster. A purely passive evolution model is also shown, assuming a formation redshift $z_{\rm F} = 5$. Middle panel: the intrinsic color scatter, having removed the mean slope of the C-M relation in each cluster and the contribution of photometric errors. The intrinsic scatter of Coma galaxies is shown for reference. Bottom panel: the redshift evolution of the slope of the ("blue"$-K$) $-$ $K$ C-M relation, relative to the slope of the corresponding relation for galaxies in Coma.

also to the color dispersion within a cluster, demonstrating that the tightness of the C-M (and FP) relation in low-$z$ clusters cannot be due to a conspiracy of age and metallicity being anticorrelated (as advocated e.g., by Worthey, Trager & Faber 1995). If so, the color dispersion would rapidly increase with redshift, contrary to what is seen in clusters up to $z \sim 1$ (see Figure 8).

4.1.2 THE LUMINOSITY FUNCTION A cross check of the high formation redshift of ETGs can be provided by looking at their luminosity in distant clusters. If ETGs evolve passively, following a pure luminosity evolution, then their luminosities should increase with increasing redshift by an amount that depends on the formation redshift and on the slope of the IMF.

Initial attempts to detect the expected brightening of the characteristic luminosity ($M^*$) of the luminosity function (LF) were inconclusive, as Barger et al. (1998) failed to detect any appreciable change between clusters at $z = 0.31$ and $z = 0.56$, possibly owing to the small redshift baseline. On the other hand, comparing the LF of $z \sim 0$ clusters to the LF of a sample of 8 clusters at

$0.40 < z < 0.48$ Barrientos & Lilly (2003) found a brightening of the characteristic luminosity $M^*$ consistent with passive evolution and high formation redshift, also in agreement with the $(U-V)$ color evolution of the red sequence. In a major cluster survey, De Propris et al. (1999) explored the evolution of the observed $K$-band LF in 38 clusters with $0.1 < z < 1$, and compared the results to the Coma LF. With this much larger redshift baseline, De Propris et al. found the trend of $K^*$ with redshift to be consistent with passive evolution and $z_{\rm F}\gtrsim 2$. They pointed out the agreement with the results based on the color evolution of the red sequence galaxies, but emphasized that this behavior of the LF implies that "not only their stellar population formed at high redshift, but that the assembly of the galaxies themselves was largely complete by $z \sim 1$". Kodama & Bower (2003) and Toft, Soucail, & Hjorth (2003) came to the same conclusions by studying the $K$-band LF of (respectively two and one) clusters at $z \sim 1$. Breaking the $z = 1$ barrier, Toft et al. (2004) constructed a very deep $K$-band LF of a rich RDCS cluster at $z = 1.237$, and concluded that the most massive ellipticals that dominate the top end of the LF were already in place in this cluster. They compared the cluster $K$-band LF (corresponding to the rest-frame $z$-band LF) to the $z$-band LF of local clusters (Popesso et al. 2005) and derived a brightening by $\sim 1.4$ mag in the rest-frame $z$-band characteristic magnitude, indeed as expected from pure passive evolution. Toft and colleagues also found a substantial deficit of fainter ETGs, which could be seen as a manifestation of the down-sizing effect in a high redshift cluster, a hint of which was also noticed in other clusters at $z \sim 0.8$ (De Lucia et al. 2004).

However, a more complete study of 3 rich clusters at $1.1\lesssim z\lesssim 1.3$, including the $z = 1.237$ cluster studied by Toft et al. (2004), did not produce evidence of a down-sizing effect, down to at least 4 magnitudes below $K^*$ (Strazzullo et al. 2006). This study confirmed the brightening of $M^*_{\rm z}$ and $M^*_{\rm K}$ by $\sim 1.3$ mag, consistent with passive evolution of a population that formed at $z\gtrsim 2$, and showed that the massive galaxies were already fully assembled at $z \sim 1.2$, at least in the central regions of the 3 clusters.

4.1.3 THE KORMENDY RELATION An alternative way of detecting the expected brightening of old stellar populations at high redshift is by tracing the evolution of the Kormendy relation, which became relatively easy only after the full image quality of HST was restored. Thus, from HST data, the ETGs in a cluster at $z = 0.41$ were found brighter by $\Delta M_{\rm K} = 0.36 \pm 0.14$ mag (Pahre, Djorgovski, & de Carvalho 1996) or by $0.64 \pm 0.3$ mag (Barrientos, Schade, & Lopez-Cruz 1996) with respect to local galaxies, consistent (within such large errors) with passive evolution of an old, single-burst stellar population. Schade et al. (1996) using excellent-seeing CFHT (Canada-France-Hawaii Telescope) imaging data for 3 clusters at $z = 0.23,\ 0.43$ and 0.55 detected a progressive brightening in galaxy luminosity at a fixed effective radius that once more was estimated to be consistent with passive evolution and formation at high redshift. No differential evolution with respect to ETGs in the cluster surrounding fields was detected.

Turning to HST data, a systematic brightening in the Kormendy relation, again consistent with passive evolution and high formation redshift, was found by several other groups, eventually reaching redshifts $\sim 1$ (see Schade, Barrientos, & Lopez-Cruz 1997, Barger et al. 1999, Ziegler et al. 1999, Holden et al. 2005a, Pasquali et al. 2006).

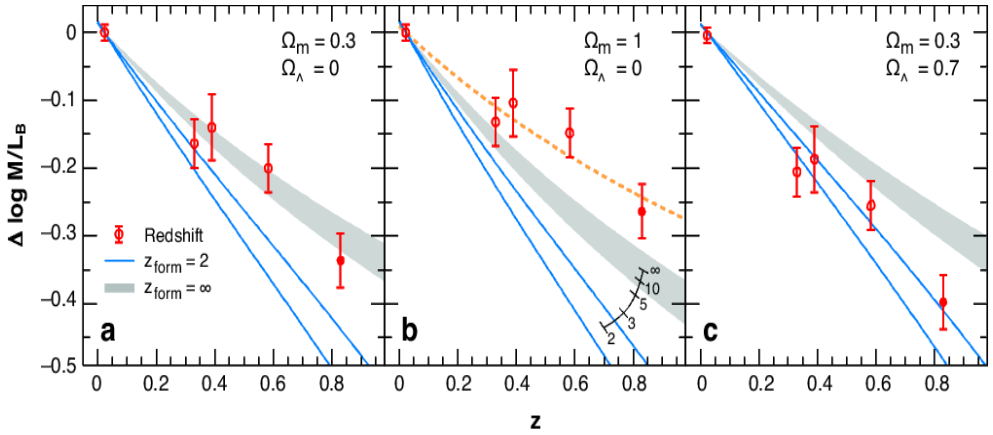


Figure 9: The data points show the redshift evolution of the $M/L_{\rm B}$ ratio of cluster elliptical galaxies as inferred from the shifts of the fundamental plane. The lines refer to the evolution of the $M/L_{\rm B}$ ratio for stellar populations with a Salpeter initial mass function (IMF) ($s = 2.35$) and formation redshifts as indicated in the left –and middle– panel. The comparison is made for three different cosmologies. The dotted line in the middle panel shows a model with $z_{\rm F} = \infty$ and a steep IMF ($s = 3.35$). From van Dokkum et al. 1998).

4.1.4 THE FUNDAMENTAL PLANE Besides the high spatial resolution, constructing the FP of high redshift cluster (and field) galaxies requires moderately high-resolution spectroscopy (to get $\sigma$), hence a telescope with large collective area. With one exception, for a few years this was monopolized by the Keck Telescope, and FP studies of high-$z$ ellipticals first flourished at this observatory. In a crescendo toward higher and higher redshifts, the FP was constructed for clusters at $z = 0.39$ (van Dokkum & Franx 1996), $z = 0.58$ (Kelson et al. 1997), $z = 0.83$ (van Dokkum et al. 1998, Wuyts et al. 2004 ), and finally at $z = 1.25$ and 1.27 (Holden et al. 2005b, van Dokkum & Stanford 2003). The early exception was the heroic study of two clusters at $z = 0.375$ using the 4m-class telescopes at ESO (NTT) and Calar Alto (Bender, Saglia, & Ziegler 1997, Bender, Ziegler, & Bruzual 1996, Bender et al. 1998).

The redshift evolution of the FP depends on a variety of factors. For passive evolution the FP shifts by amounts that depend on a combination of IMF slope, formation redshift, and cosmological parameters. A systematic trend of the IMF slope with galaxy mass would cause the FP to rotate with increasing redshift (Renzini & Ciotti 1993), as it would do for a similar trend in galaxy age. An age dispersion ($\Delta t$) would cause the scatter perpendicular to the FP to increase with redshift, as, for fixed $\Delta t$, $\Delta t/t$ increases for increasing redshift, i.e. decreasing galaxy age ($t$). Clearly, the behavior of the FP with redshift can give a wealth of precious information on the formation of ellipticals, their stellar populations, and to some extent on cosmology also (Bender et al. 1998).

All the quoted FP studies of high-$z$ clusters conclude that the FP actually shifts nearly parallel to itself by an amount that increases with redshift and is consistent with the passive evolution of stellar populations that formed at high redshifts. The FP shifts imply a decrease of the rest-frame $M/L$ ratio $\Delta\log M/L_{\rm B} \simeq -0.46z$ (van Dokkum & Stanford 2003), but – as emphasized above – the formation redshift one can derive from it depends on both cosmology and the IMF. Figure 9 illustrates the dependence on the adopted cosmology. Note that for the "old

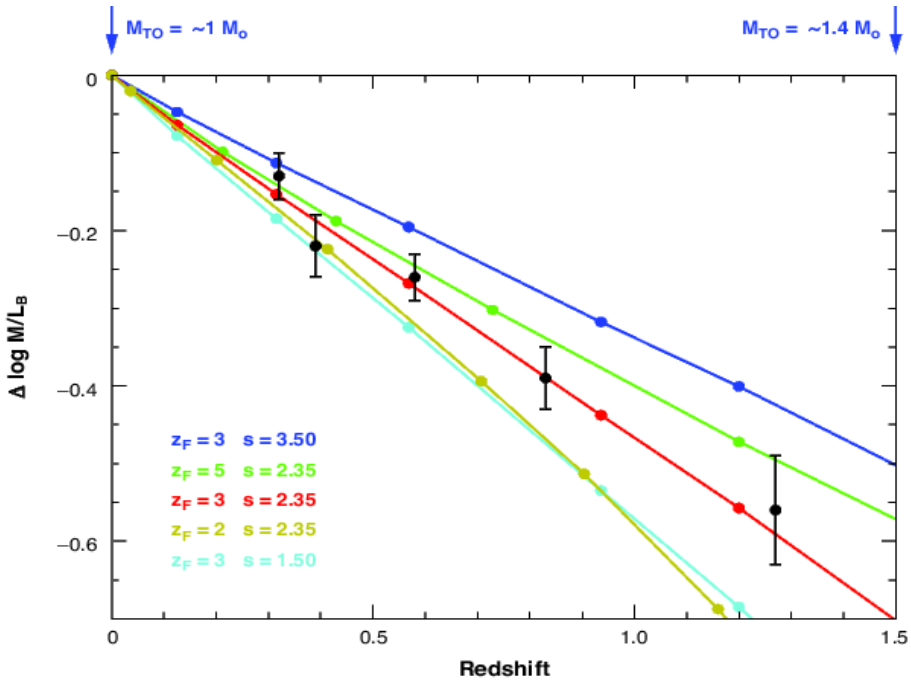


Figure 10: The evolution with redshift of the $M_*/L_{\rm B}$ ratio of simple stellar populations of solar metallicity and various initial mass function slopes ($dN \propto M^{-s}dM$) and formation redshifts, as indicated. The curves are normalized to their value at $z = 0$. Concordance cosmology ($\Omega_{\rm m} = 0.3$, $\Omega_\Lambda = 0.7$, $H_\circ = 70$) is adopted. The data points (from van Dokkum & Stanford 2003) refer to the shifts in the fundamental plane locations for clusters at various redshifts. Note that for such high formation redshifts the stellar mass at the main sequence turnoff is $\sim 1.4\,M_\odot$ at $z = 1.5$ and $\sim 1.0\,M_\odot$ at $z = 0$, as indicated by the arrows. Adapted from Renzini (2005).

standard" cosmology ($\Omega_{\rm M} = 1$) galaxies would be older than the universe and therefore the observed FP evolution can effectively rule out this option (see also Bender et al. 1998).

Figure 10 shows the effect of the IMF slope and formation redshift on the expected evolution of the $M/L_{\rm B}$ ratio. The redshift range $z = 0$ to 1.5 only probes the IMF between $\sim 1$ and $\sim 1.4\,M_\odot$, which correspond to the masses at the main sequence turnoff $M_{\rm TO}$ of oldest populations at $z = 0$ (age $\sim 13$ Gyr, $M_{\rm TO} \simeq M_\odot$) and of those at $z = 1.5$ (age $\sim 4.5$ Gyr and $M_{\rm TO} \simeq 1.4\,M_\odot$). Together, Figure 9 and 10 illustrate the formation redshift/IMF/cosmology degeneracies in the FP diagnostics. However, the cosmological parameters are now fixed by other observational evidences, whereas the formation redshift as determined by the color evolution of the cluster red sequence is independent of the IMF slope. In summary, in the frame of the current concordance cosmology, when combining the color and FP evolution of cluster ellipticals one can conclude that the best evidence indicates a formation redshift $z_{\rm F} \sim 3$ and a Salpeter IMF slope in the pertinent stellar mass range ($1 < M < 1.4\,M_\odot$).

The fact that the cluster FP does not appreciably rotate with increasing redshift is documented down to $\sigma \sim 100\,{\rm km\ s^{-1}}$ for clusters out to $z \sim 0.3 - 0.4$ (lookback time $\sim 4$ Gyr) (Kelson et al. 2000, van Dokkum & Franx 1996) and down to $\sigma \sim 150\,{\rm km\ s^{-1}}$ out to $z \sim 0.8$ (lookback time $\sim 7$ Gyr) (Wuyts et al.

2004). If the large age trends with $\sigma$ derived in some of the studies using the Lick/IDS indices were real (see Section 3.1), this would result in a very large rotation of the FP in these clusters. For example, if age were to increase along the FP from 5.5 Gyr to 13 Gyr (at $z = 0$, and for $\sigma = 100$ and 320 km s$^{-1}$, respectively, see Nelan et al. 2005), then at a lookback time of 4 Gyr ($z \sim 0.4$) the younger population would have brightened by $\Delta M_{\rm B} \sim 1.33$ mag, and the older one only by $\sim 0.46$ mag (using models from Maraston 2005), which results in a FP rotation of $\sim 0.9$ mag in surface brightness. Alternatively, the much shallower age$-\sigma$ relation derived by Thomas et al. (2005) implies an age increase from $\sim 9.5$ Gyr to $\sim 11.5$ Gyr for $\sigma$ increasing from 180 to 350 km s$^{-1}$, which implies a rotation of the FP by $\sim 0.36$ mag in surface brightness by $z = 0.8$, which is still consistent with the hint that in fact there may be a small FP rotation in a cluster at this redshift (Wuyts et al. 2004).

The scatter about the FP of clusters also remains virtually unchanged with increasing redshift, however some of the claimed age-metallicity anticorrelations derived from the Lick/IDS indices would result in a dramatic increase of the scatter with redshift, causing the FP itself to rapidly blur away.

4.1.5 THE LINE INDICES The intermediate resolution spectra used for constructing the FP of distant cluster ETGs, were also used to measure age-sensitive line indices that can provide further constraints on the formation epoch. Thus, Bender, Ziegler, & Bruzual (1996) and Ziegler & Bender (1997) measured the Mg$b$ index of 16 ETGs in their two clusters at $z = 0.375$, and found that the Mg$b - \sigma$ relation was shifted toward lower values of the index. From such differences in Mg$b$ index, Ziegler & Bender inferred that the age of the $z = 0.375$ galaxies is about two thirds of that of ETGs in Coma and Virgo. Therefore, $t(z = 0) - t_{\rm F} = 1.5 \times [t(z = 0.375) - t_{\rm F}]$, where $t$ is the cosmic time and $t_{\rm F}$ the cosmic time when the local and distant cluster ETGs formed (which is assumed to be the same). Adopting the $t - z$ relation for the concordance cosmology, one derives $t_{\rm F} \sim 1.7$ Gyr, corresponding to $z_{\rm F} \gtrsim 3$.

From the strength of the Balmer absorption lines ($H_\delta$ and $H_\gamma$) as age indicators, Kelson et al. (2001) used data for several clusters up to $z = 0.83$ and were able to set a lower limit to the formation redshift $z_{\rm F} \gtrsim 2.5$, consistent with the above result from the Mg$b$ index.

In summary, the study of the stellar populations in ETGs belonging to distant clusters up to $z \sim 1.3$ have unambiguously shown that these objects have evolved passively from at least $z \sim 2 - 3$. This came from the color, line strength, and luminosity evolution. Moreover, the brightest cluster members at $z \sim 1 - 1.3$ and the characteristic luminosity of the LF appear to be brighter than their local counterpart by an amount that is fully consistent with pure passive evolution, indicating that these galaxies were already fully assembled at this high redshift. This may not have been the case for less massive galaxies, as their counts may be affected by incompleteness.

4.1.6 CAVEATS Although it is well established that ETGs in distant clusters are progenitors to their local analogs and formed at high redshift, some caveats are nevertheless in order. First, as frequently emphasized, the evidence summarized above only proves that at least some cluster galaxies evolved passively from $z \gtrsim 1$ to the present, but other local ETGs may have $z \sim 1$ progenitors that would not qualify as ETGs at that redshift, either morphologically or photometrically. This "progenitor bias" (e.g., van Dokkum & Franx 1996) would therefore pre-

vent us from identifying all the $z \sim 1$ progenitors of local cluster ETGs, some of which may well be still star forming. Second, the slope of the FP is progressively less accurately constrained in higher and higher redshift clusters, because the central velocity dispersion has been measured only for very few cluster members (generally the brightest ones). Third, it is always worth recalling that all luminosity-weighted ages tend to be biased toward lower values by even minor late episodes of star formation. Last, stellar population dating alone only shows when stars were formed, not when the galaxy itself was assembled and reached its observed mass.

### *4.2 Field versus Cluster Ellipticals up to $z \sim 1$*

In the local universe field ellipticals show small, yet detectable differences compared to their cluster counterpart, being possibly $\sim 1$ Gyr younger, on average. This $\Delta t$ difference, if real, should magnify in relative terms and become more readily apparent when moving to high redshift ($\Delta t/t$ is increasing). Using the color evolution of the red sequence and the shift of the FP with redshift, progress in investigating high$-z$ ETGs in the field has been dramatic in recent years, along with the cluster versus field comparison.

Schade et al. (1999) selected ETGs by morphology from the Canada-France Redshift Survey (CFRS, Lilly et al. 1995a,b) and Low Dispersion Survey Spectrograph (LDSS) redshift survey (Ellis et al. 1996), and constructed the rest-frame $(U-V)$ C-M relation for field ETGs in the $0.2 < z < 1.0$ range. They found that the C-M relation becomes progressively bluer with redshift, with $\Delta(U-V) \simeq -0.68 \pm 0.11$ at $z = 0.92$ with respect to the relation in Coma, accompanied by a brightening by $\sim 1$ mag in the rest-frame $B$ band, as derived from the Kormendy relation. To be consistent with the color evolution, this brightening should have been much larger than observed if the color evolution were due entirely to the passive evolution of stellar populations formed at high $z$. Thus, Schade and colleagues reconciled color and luminosity evolution by invoking a residual amount of star formation (adding only $\sim 2.5\%$ of the stellar mass from $z = 1$ to the present), yet enough to produce the observed fast color evolution. Support for such an interpretation comes from about one third of the galaxies exhibiting weak [OII] emission, which indicates that low-level star formation is indeed fairly widespread. The rate of luminosity evolution was found to be identical to that of cluster ellipticals at the same redshifts, hence no major environmental effect was detected besides the mentioned low level of star formation and a color dispersion slightly broader than in clusters at the same redshift.

With COMBO-17, the major imaging survey project undertaken with the ESO/MPG 2.2m telescope, Wolf et al. (2003) secured deep optical imaging in 17 broad and intermediate bands over a total 0.78 square degree area, from which Bell et al. (2004b) derived photometric redshifts accurate to within $\delta z \sim 0.03$. The bimodality of the C-M relation, so evident at $z \sim 0$ (e.g., Baldry et al. 2004), clearly persists all the way to $z \sim 1.1$ in the COMBO-17 data, and this allowed Bell and colleagues to isolate $\sim 5,000$ "red sequence" ETGs down to $R < 24$. As mentioned above, $\sim 85\%$ of such color-selected galaxies appear also morphologically early-type on the ACS images of the GEMS (Galaxy Evolution from Morphology and SED) survey (Rix et al. 2004, Bell et al. 2004a). The rest-frame $(U-V)$ color of ETGs in the COMBO-17 survey evolves by a much smaller amount than that reported by Schade et al. (1999) for the morphologically-

selected ETGs, i.e., by only $\sim 0.4$ mag between $z = 0$ and 1, as expected for an old stellar population that formed at high redshift ($z_{\rm F} \gtrsim 2$). This color evolution is also in agreement with the $\sim 1.3$ mag brightening of the characteristic luminosity $M^*_{\rm B}$ in the Schechter fit to the observed LF. Thus, when comparing only the color and $M^*_{\rm B}$ evolution, the field ETGs in the COMBO-17 sample seem to evolve in much the same fashion as their cluster counterparts. Using COMBO-17 data and GEMS HST/ACS imaging, McIntosh et al. (2005) studied a sample of 728 morphology- and color-selected ETGs, finding that up to $z \sim 1$ the Kormendy relation evolves in a manner that is consistent with the pure passive evolution of ancient stellar populations.

From deep Subaru/Suprime-Cam imaging over a 1.2 deg$^2$ field [covered by the Subaru-XMM Deep Survey (SXDS)], Kodama et al. (2004) selected ETGs for having the $R - z$ and $i - z$ colors in a narrow range as expected for passively evolving galaxies in the range $0.9 \lesssim z \lesssim 1.1$, and the sampled population included both field and cluster ETGs. They found a deficit of red galaxies in the C-M sequence $\sim 2$ mag fainter than the characteristic magnitude (corresponding to stellar masses below $\sim 10^{10} M_\odot$). Less massive galaxies appear to be still actively star-forming, while above $\sim 8 \times 10^{10} M_\odot$ galaxies are predominantly passively evolving. This was interpreted as evidence for down-sizing in galaxy formation (à la Cowie et al. 1996), with massive galaxies having experienced most of their star formation at early times and being passive by $z \sim 1$, and many among the less massive galaxies experience extended star formation histories.

In a comprehensive study also based on deep, wide-field imaging with the Suprime-Cam at the Subaru Telescope, Tanaka et al. (2005) obtained photometric redshifts based on four or five optical bands and constructed the C-M relations for the two clusters (at $z = 0.55$ and 0.83) included in the field, and for their extended environment. Tanaka and colleagues further distinguished galaxies in the cluster environment as belonging either to recognized "groups", or otherwise to the "field". The results are shown in Figure 11, where the various plots allow one to visually explore trends with redshift for given environment, or with environment for given redshift. The red sequence appears already in place in the "field" in the highest redshift sample, but no clear color bimodality is apparent. (Note that COMBO-17 does find bimodality at this redshift, possibly due to its photometric redshifts based on many more bands being more accurate.) The color bimodality is instead clearly recognizable in the $z = 0.55$ "field" sample. At higher environmental densities (labelled "group") the C-M relation of the red sequence is clearly recognizable already in the $z = 0.83$ sample, and even more so in the "cluster" sample. Tanaka and colleagues argue that the bright and the faint ends of the red sequence are populated at a different pace in all three environments; the more massive red galaxies are assembled first, i.e., the C-M relation grows from the bright end to the faint end in all three environments (not in the opposite way, as one may naively expect in a hierarchical scenario), which is interpreted in terms of down-sizing. Note also that the faint end appears to be well in place in "clusters" at $z = 0$ while virtually still lacking in the field (see also Popesso et al. 2005). Using HST/WFPC2 imaging over a $\sim 30$ arcmin$^2$ field including the same $z = 0.83$ cluster, Koo et al. (2005) were able to measure the rest-frame $(U - B)$ colors of the sole bulge component of 92 galaxies with $M_{\rm B} < -19.5$, part in the cluster itself, part in the surrounding field. Their very

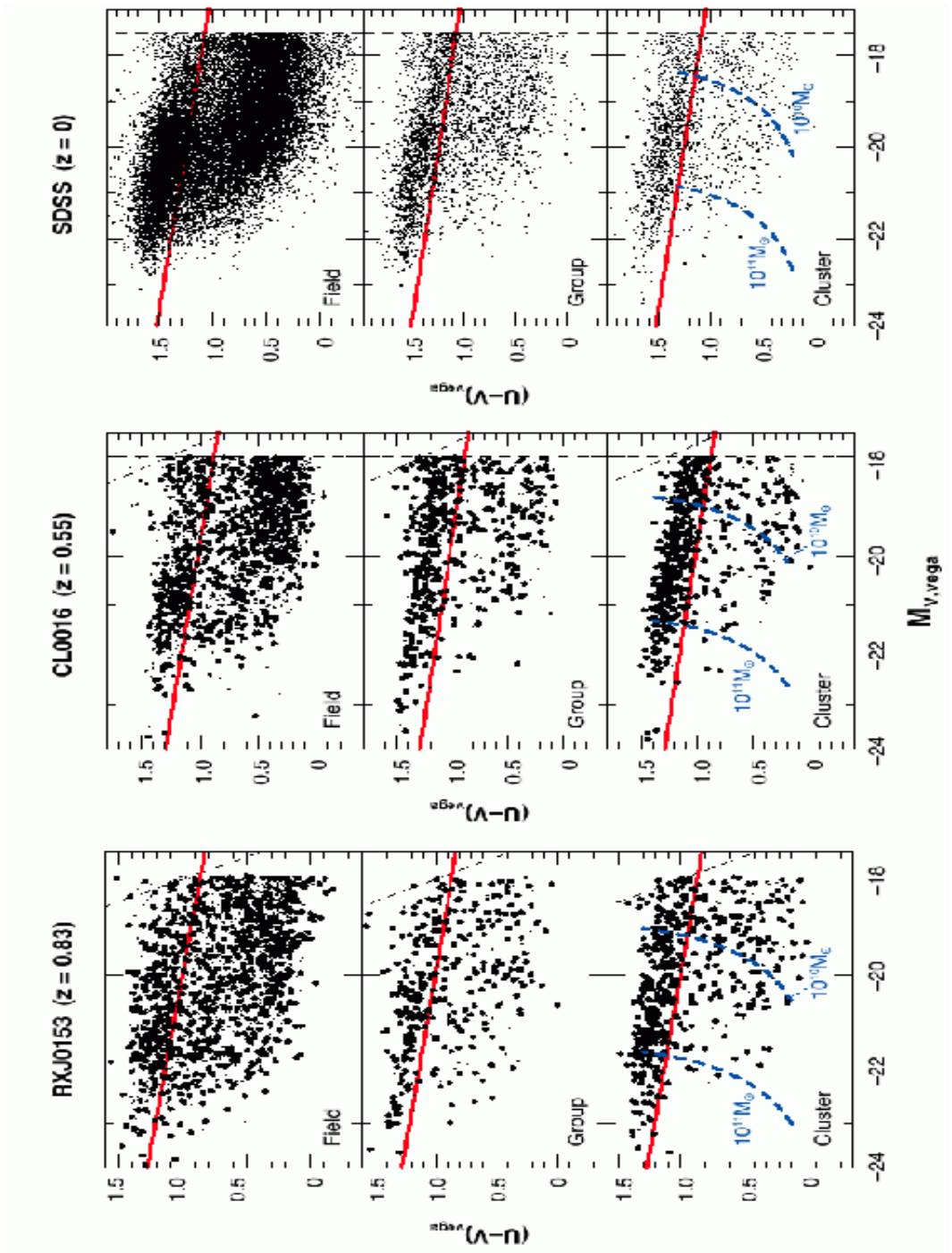


Figure 11: The C-M relations of two high redshift clusters and their surrounding fields at progressive lower density (labelled "group" and "field") are compared to their local counterparts from the Sloan Digital Sky Survey. The red line marks the adopted separation between the red sequence galaxies, and the blue, star-forming galaxies. In the cluster panels the blue dashed lines show the approximate location of galaxies with stellar mass of $10^{10}$ (right) and $10^{11} M_{\odot}$ (left). From Tanaka et al. (2005).

red color does not show any environmental dependence, suggesting similarly old ages and high formation redshifts.

The public delivery of the Hubble Deep Field data (HDF, Williams et al. 1996) spurred several studies of field ETGs. Thus, Fasano et al. (1998) applied the Kormendy relation to a sample of morphologically selected ETGs in HDF-North and estimated an increase of the surface brightness at a fixed effective radius that was consistent with a high formation redshift ($z_{\rm F} \sim 5$), according to the galaxy models by Bressan, Chiosi & Fagotto (1994) and Tantalo et al. (1996).

Although the LF and the C-M and Kormendy relations had already given useful indications on the analogies and differences between cluster and field ETGs, major progress came with the study of the differential evolution (field versus cluster) of the FP with redshift. In early studies, no field/cluster difference had clearly emerged at $z = 0.3$ (Treu et al. 1999), $z \sim 0.4$ (Treu et al. 2001), $z = 0.55$ (van Dokkum et al 2001), and $z = 0.66$ (Treu et al. 2002). But already at these modest redshifts there were hints that the brightest, most massive ETGs in the field closely follow the FP evolution of their cluster counterparts, while less massive ETGs (especially S0's) appear to evolve slightly faster, and hence look younger. This was more accurately quantified for morphologically-selected ETGs up to $z \sim 1$ in the HDF-North by van Dokkum & Ellis (2003), showing a field versus cluster difference $\Delta \ln M/L_{\rm B} = -0.14 \pm 0.13$ in the FP. This implies that field ETGs are on average younger by only $16\% \pm 15\%$ at $< z >= 0.88$. Van Dokkum & Ellis also inferred that the bulk of stellar mass in the observed ETGs must have formed at $z \gtrsim 2$ even in the field, with only minor star formation at lower redshifts. Then, moving to the wider GOODS (Great Observatories Origin Deep Survey)-South field (Giavalisco et al. 2004a), van der Wel et al. (2004, 2005a) constructed the FP for a total of 33 color and morphology-selected ETGs at $0.60 < z < 1.15$, using intermediate resolution spectra taken at the ESO Very Large Telescope (VLT). They also found the most massive galaxies ($M_* > 2{\times}10^{11} M_\odot$) to behave much like their cluster analogs at the same redshifts, while less massive galaxies appeared to be substantially younger. Moreover, all these studies noted the higher proportion of weak [OII] emitters among the field ETGs ($\sim 20\%$) compared to their cluster counterparts, as well as the higher proportion of galaxies with strong Balmer lines (the K+A Galaxies).

The main limitations of all these early studies was in the small number of objects observed at each redshift, which must go a long way toward accounting for occasional discrepancies in the results. In a major effort to overcome this limitation, Treu et al. (2005a,b) obtained high-resolution spectra at the Keck telescope for 163 morphologically-selected ETGs in the GOODS-North field, which were distributed over the redshift range $0.2 < z < 1.2$. The main results of this study are displayed in Figure 12, showing that the most massive ellipticals in the field do not differ appreciably from their cluster analogs in having luminosity-weighted ages implying $z_{\rm F} \gtrsim 3$. However, the lower the mass the larger the dispersion in the $M/L_{\rm B}$ ratio, with a definite trend toward lower values with decreasing mass, implying lower and lower formation redshift. This demonstrates that completion of star formation in field galaxies proceeds from the most massive to the less massive ones, as is indeed expected from the down-sizing effect (Cowie et al. 1996, Kodama et al. 2004) and is consistent with the scenario shown in Figure 6. This systematic trend in the $M/L$ ratio with galaxy mass results in a "rotation" of the FP with increasing redshift, as less massive galaxies evolve faster in luminosity compared to the more massive, older ones (but one should beware of possible

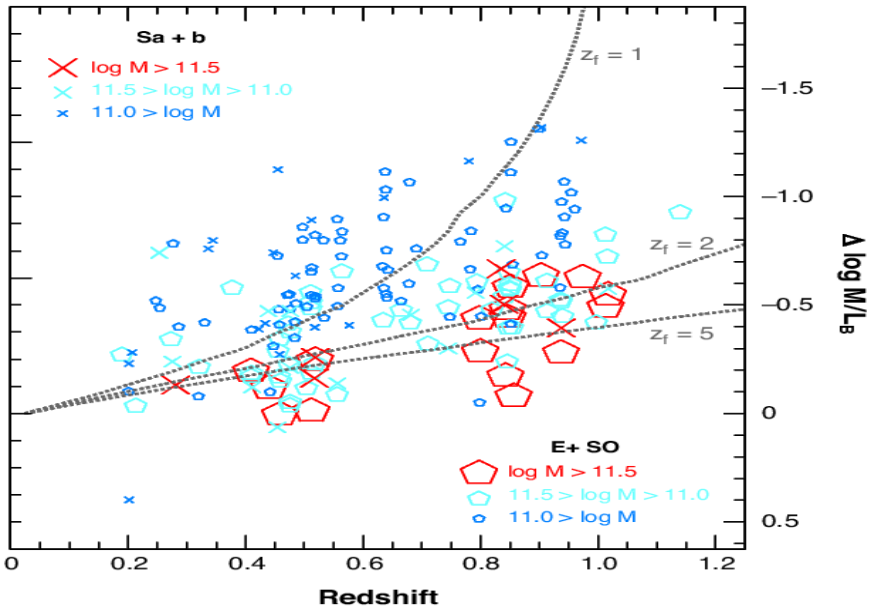


Figure 12: The offset $\Delta\log M/L_{\rm B}$ from the fundamental plane of cluster ellipticals at $z\sim 0$ for the early-type galaxies in the GOODS-North field (from Treu et al. 2005b). Different symbols are used for early-type (E+S0) galaxies and bulges in late-type (Sa+Sb) galaxies, as well as for the various stellar mass ranges as indicated. The dotted lines are labelled by various formation redshifts.

Malmquist bias). This result confirms early hints for a modest rotation of the FP of field ETGs with redshift, as also does a study of the FP of 15 ETGs at $0.9\lesssim z\lesssim 1.3$ by di Serego Alighieri et al. (2005), a sample drawn from the K20 survey (Cimatti et al. 2002b). Figure 13 shows the FP for the combined Treu et al. (2005b) and di Serego Alighieri et al. (2005) samples of ETGs with $<z>=1.1$, where the rotation with respect to the Coma FP is apparent. Note that a similar FP rotation in two clusters at $z=0.83$ and 0.89 has been recently unambiguously detected by Jørgensen et al. (2006), having extended the $\sigma$ measurements below $\sim 100$ km s$^{-1}$. Somewhat at variance with the FP studies reported above was the Deep Groth Strip Survey result (Gebhardt et al. 2003), in which no difference in the slope was found up to $z\sim 1$ compared to the local FP (hence no downsizing), which was coupled to a much faster luminosity evolution compared to all other results. Treu et al. (2005b) discuss the possible origins of the discrepancy, and attribute it to a combination of selection bias, small number statistics, and relatively low S/N spectra.

From population synthesis models one expects the rate of evolution of the $M/L$ ratio to be slower at longer wavelengths compared to the $B$ band, because it is less affected by the main sequence turnoff moving to cooler temperatures with increasing age. This expectation was qualitatively confirmed by van der Wel et al. (2005b), who found $\Delta\ln(M/L_{\rm B})=-(1.46\pm 0.09)z$ and $\Delta\ln(M/L_{\rm K})=-(1.18\pm 0.1)z$, which appears to be in agreement with the prediction of some models (Maraston 2005), but not of others (Bruzual & Charlot 2003), possibly owing to the different treatment of the AGB contribution.

Instead of measuring central velocity dispersions directly, Kochanek et al. (2000) and Rusing and Kochanek (2005) estimated them from the lens geometry for a sample of (field) lensing ETGs at $0.2\lesssim z\lesssim 1$. The resulting FP shifts

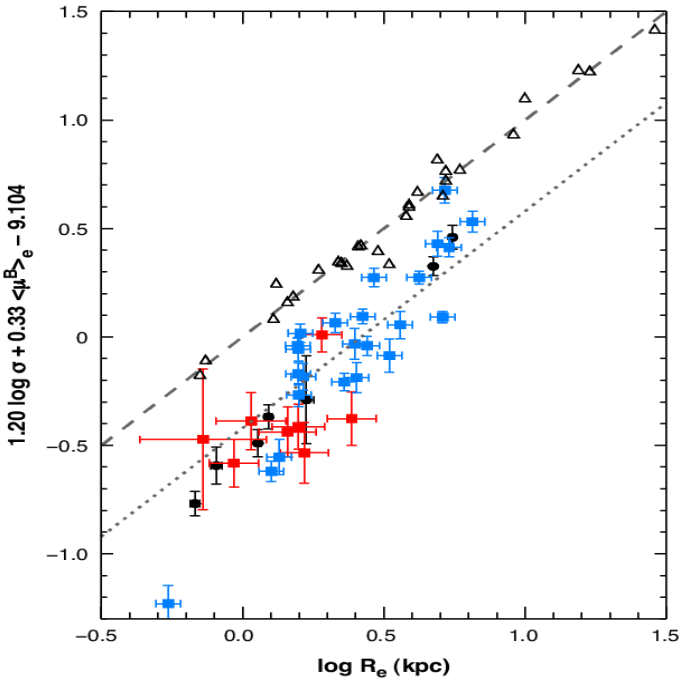


Figure 13: An edge-on view of the fundamental plane for field ETGs at $z \sim 1.1$ from di Serego Alighieri et al. (2005, red squares and black circles) and Treu et al. (2005b, green squares). Open triangles refer to the Coma ellipticals from Jørgensen, Franx, & Kjærgaard (1995) and the dashed line is a best fit to the data. The dotted line is shifted parallel to the dashed line by an amount in surface brightness corresponding to the observed shift of the fundamental plane of galaxy clusters (i.e., $\Delta M/L_{\rm B} = -0.46z$, van Dokkum & Stanford 2003). The effective surface brightness in the $B$ band ($\mu_{\rm e}^{\rm B}$) is in magnitudes per arcsec$^2$.

appear to be similar to those of cluster ETGs, although with more scatter, and indicate $< z_{\rm F} > \gtrsim 1.5$ for the bulk of the stars in the lensing galaxies.

In summary, like at low redshifts, also at $z \sim 1$ there appear to be small detectable differences between ETGs in high- and low-density regions, but such differences are more evident for faint/low-mass galaxies than for the bright ones.

### *4.3 Ellipticals Beyond $z \sim 1.3$*

Up to $z \sim 1.3$ the strongest features in the optical spectrum of ETGs are the CaII H&K lines and the 4000 Å break. But at higher redshifts these features first become contaminated by OH atmospheric lines, and then move to the near-IR, out of reach of CCD detectors. The lack of efficient near-IR multi-object spectrographs (even in just the $J$ band) has greatly delayed the mapping of the ETG population beyond $z \sim 1.3$. Thus, for almost a decade the most distant spectroscopically confirmed old spheroid was an object at $z = 1.55$ selected for being a radiogalaxy (Dunlop et al. 1996, Spinrad et al. 1997). The spectral features that made the identification possible included a set of FeII, MgII and MgI lines in the rest-frame near-UV, in the range of $\sim 2580 - 2850$ Å, which is typical of F-type stars. The UV Fe-Mg feature offers at once both the opportunity to measure the redshift, and to age-date the galaxy, because it appears only in populations that have been passively evolving since at least a few $10^8$ years. It

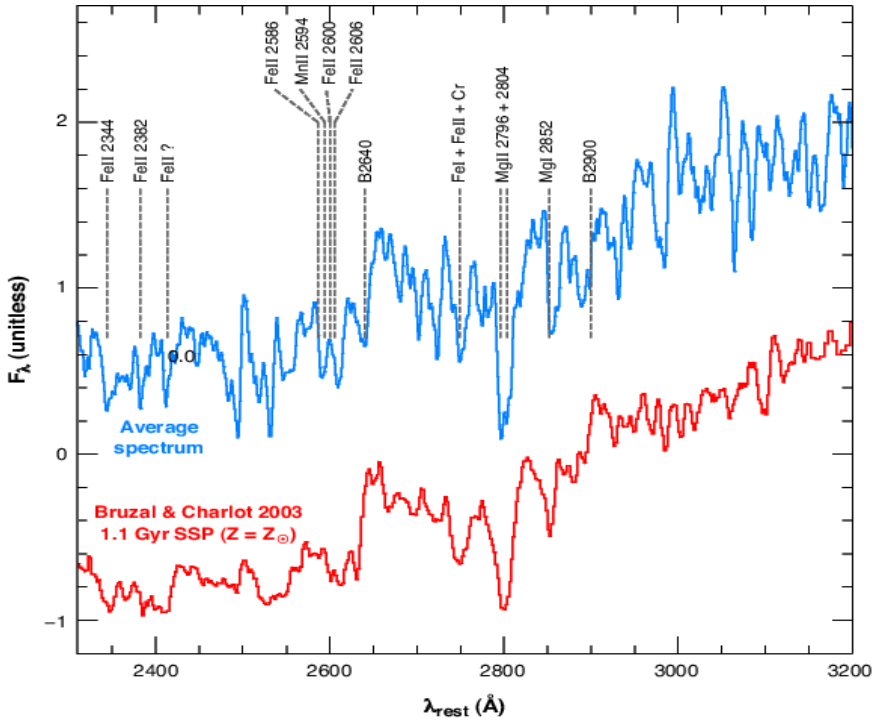


Figure 14: The rest-frame coadded spectrum of the four passively evolving galaxies at $1.6 < z < 1.9$ with the identification of the main spectral features (blue spectrum). The spectrum from Bruzual & Charlot (2003) for a 1-Gyr-old SSP (simple stellar population) model of solar metallicity is also shown (red spectrum). (From Cimatti et al. 2004)

has been also used to age-date local ETGs (e.g., Buson et al. 2004). Thus, using this feature, Spinrad and colleagues inferred an age of $\sim 3.5$ Gyr, implying $z_F > 5$ (even in modern cosmology).

This record for the highest redshift ETG was eventually broken by Glazebrook et al. (2004) and Cimatti et al. (2004), using the same features in the rest-frame UV (see Figure 14). They reported the discovery of, respectively, five passively evolving galaxies at $1.57 \lesssim z \lesssim 1.85$, and four other such objects at $1.6 \lesssim z \lesssim 1.9$. All being brighter than $K = 20$, these galaxies are quite massive ($M \gtrsim 10^{11} M_\odot$), and hence would rank among the most massive galaxies even in the local universe. This suggests that they were (almost) fully assembled already at this early epoch, and having been passive since at least $\sim 1.1$ Gyr had to form at redshift $\gtrsim 2.7$ . The four objects found by Cimatti and colleagues are included in the GOODS-South field, and the GOODS deep HST/ACS imaging showed that two objects are definitely elliptical galaxies, and the two others are likely to be S0's.

Though breaking the old redshift record was certainly an exciting result, perhaps far more important was the discovery that the surface density of $z > 1.5$ ETGs is indeed much higher than one would have expected from just the single object found by Dunlop et al. (1996). Indeed, this galaxy was selected from a catalog of radiogalaxies covering a major fraction of the whole sky, whereas the nine galaxies in the Cimatti and colleagues and Glazebrook and colleagues samples come from a combined area of only 62 arcmin$^2$.

Further identifications of very high redshift ETGs used this UV feature: Mc-

Carthy et al. (2004) reported the discovery of 20 ETGs with $1.3 \lesssim z \lesssim 2.15$ and $K < 20$ as part of the Gemini Deep Deep Survey (GDDS) (including the 5 galaxies from Glazebrook et al. 2004). Within the $\sim 11$ arcmin$^2$ area of the Hubble Ultra Deep Field (HUDF, Beckwith et al. in preparation), Daddi et al. (2005b) identified 7 ETGs with $1.39 \lesssim z \lesssim 2.5$ using their HST/ACS grism spectra. For all these objects the stellar mass derived from the spectral energy distribution (SED, typically extending from the $B$ to the $K$ band) is in excess of $\sim 10^{11} M_{\odot}$. Over the same field, Yan et al. (2004) identify 17 objects with photometric redshifts between 1.6 and 2.9, whose SED can be best fit by a dominant $\sim 2$ Gyr old stellar population, superimposed to a low level of ongoing star formation.

Rather than digging deep into small fields, Saracco et al. (2005) searched for bright high-$z$ ETGs over the $\sim 160$ arcmin$^2$ field of the MUNICS survey (Drory et al. 2001), and selected objects with $R - K > 5.3$ and $K < 18.5$ for spectroscopic follow up with the low-resolution, near-IR spectrograph on the TNG 3.5m telescope. They identified 7 ETGs at $1.3 \lesssim z \lesssim 1.7$, all with mass well in excess of $10^{11} M_{\odot}$.

Altogether, these are virtually all the spectroscopically confirmed ETGs at $z > 1.3$ known to date. Given the long integration time needed to get spectroscopic redshifts, it became clear that an effective criterion was indispensable to select high-$z$ ETG candidates. To this end, Daddi et al. (2004) introduced a robust criterion based on the $B-z$ and $z-K$ colors, that very effectively selects galaxies at $1.4 \lesssim z \lesssim 2.5$ (the so-called BzKs), and among them separates the star forming BzKs with $BzK \equiv (z-K)_{\rm AB} - (B-z)_{\rm AB} \geq -0.2$, from the passive ones, with $BzK < -0.2$ and $(z-K)_{\rm AB} > 2.5$. The criterion is primarily an empirical one, based on the spectroscopic redshifts from the K20 survey (Cimatti et al. 2002b) and other publicly available data sets. However, Daddi and colleagues showed that synthetic stellar populations of the two kinds (i.e., star forming and passive) do indeed occupy the corresponding areas in this plot, when redshifted to $1.4 < z < 2.5$. An application of the method to a 320 arcmin$^2$ field is shown in Figure 15 (Kong et al. 2006). In this latter study, it is estimated that the space density of massive and passive BzKs (with $K < 20$, stellar mass $\gtrsim 10^{11} M_{\odot}$ and $< z > \simeq 1.7$) is $20 \pm 7\%$ that of $z = 0$ ETGs within the same mass limit. Then there appears to be a sharp drop of passive BzKs beyond $z = 2$, which in part may be due to the available $B$-band data being not deep enough (Reddy et al. 2005)

Further candidate ETGs with masses up to a few $10^{11} M_{\odot}$ have been identified at even higher redshifts, such as six objects within the HUDF at a (photometric) redshift $> 2.8$ (Chen & Marzke 2004), where both the redshift and the old age are inferred from the observed break between the $J$ (F110W) and the $H$ (F160W) band being interpreted as the 4000 Å break. One of these objects is undetected in the deep GOODS optical data, but is prominent in the GOODS Spitzer/IRAC $3.5 - 8$ $\mu$m images (M. Dickinson et al., in preparation). Thus its SED shows two breaks, one between the $z$ and the $J$ band, and one between the $K$ and the 3.5 $\mu$m IRAC band. Identifying them respectively with the Lyman and Balmer breaks, the object would be placed at $z \sim 6.5$, it would be passively evolving with $z_{\rm F} > 9$, and would have the uncomfortably large mass of a few $10^{11} M_{\odot}$ (Mobasher et al. 2005). Lower redshift alternatives give much worse fits to the data, whereas the use of models with strong AGB contribution (Maraston 2005) results in a somewhat less extreme mass and formation redshift.

### *4.4 Evolution of the Number Density of ETGs to $z \sim 1$ and Beyond*

The studies illustrated so far have shown that ETGs exist up to $z \sim 1$, both in clusters and in the field, and are dominated by old stellar populations that formed at $z \gtrsim 2-3$. Moreover, a handful of ETGs has also been identified (over small fields) well beyond $z \sim 1$. Some of these ETGs appear to be as massive as the most massive ETGs in the local universe, demonstrating that at least some very massive ETGs are already fully assembled at $z \gtrsim 1$. However, the expectation is for the number of ETGs to start dropping at some redshift, when indeed entering into the star formation phase of these galaxies, or when they were not fully assembled yet. Therefore, what remained to be mapped by direct observations was the evolution with redshift of the comoving number density of ETGs, and to do so as a function of mass and environment while covering wide enough areas of the sky in order to reduce the bias from cosmic variance. Only in this way one could really overcome the so-called progenitor bias. Because deep and wide surveys require so much telescope time, progress has been slow. Cosmic variance may still be responsible for the apparent discrepancies between galaxy counts from different surveys, but occasionally the interpretation itself of the counts may be prone to ambiguities.

One of the main results of the CFRS was that the number density of red galaxies shows very little evolution over the redshift range $0 < z < 1$ (Lilly et al. 1995b). Following this study, in an attempt to map the number evolution of ETGs all the way to $z \sim 1$ , Kauffmann, Charlot, & White (1996) extracted 90 color-selected ETGs without [OII] emission from the CFRS redshift catalog. They used a $V/V_{\rm max}$ test and concluded that at $z = 1$ only $\sim 1/3$ of bright ETGs had already assembled or had the colors expected for old, pure passively evolving galaxies. However, Im et al. (1996) identified $\sim 360$ ETGs morphologically selected on archival HST images, and also conducted the $V/V_{\rm max}$ test using photometric redshifts, finding no appreciable number density evolution up to $z \sim 1$ and a brightening consistent with passive evolution. The $V/V_{\rm max}$ test was repeated – again using the CFRS sample – by Totani & Yoshii (1998) who concluded that there was no evolution in the number density up to $z \sim 0.8$, and ascribed the apparent drop at $z > 0.8$ to a color selection bias. No evolution of the space density of morphologically-selected ETGs up to $z \sim 1$ was found by Schade et al. (1999) too, who used the HST imaging of the CFRS and LDSS redshift surveys.

Several attempts to trace the evolution of the number density of morphologically-selected ETGs to the highest possible redshifts were made using HDF data. In some of these studies very little, if any, change in the space density of ETGs was found up to $z \sim 1$ (e.g., Driver et al. 1998, Franceschini et al. 1998, Im et al. 1999), or up to even higher redshifts when combining the HDF optical data with very deep near-IR data (Benitez et al 1999, Broadhurst & Bouwens 2000). These latter authors emphasized that without deep near-IR data many high-$z$ ETGs are bound to remain undetected, and that spectroscopic incompleteness beyond $z \sim 0.8$ is partly responsible for some of the previous discrepancies. Beyond $z \sim 1$ a drop in the space density of ETGs was detected in several studies including the HDF (Zepf 1997, Franceschini et al. 1998, Barger et al. 1999, Rodighiero, Franceschini, & Fasano 2001, Stanford et al. 2004). In particular, Stanford and colleagues applied the $V/V_{\rm max}$ test to a sample of 34 ETGs from the HDF-North that includes deep NICMOS imaging in the $H$ band (F160W), and concluded for a real drop at $z > 1$, but advocated the necessity to explore much wider

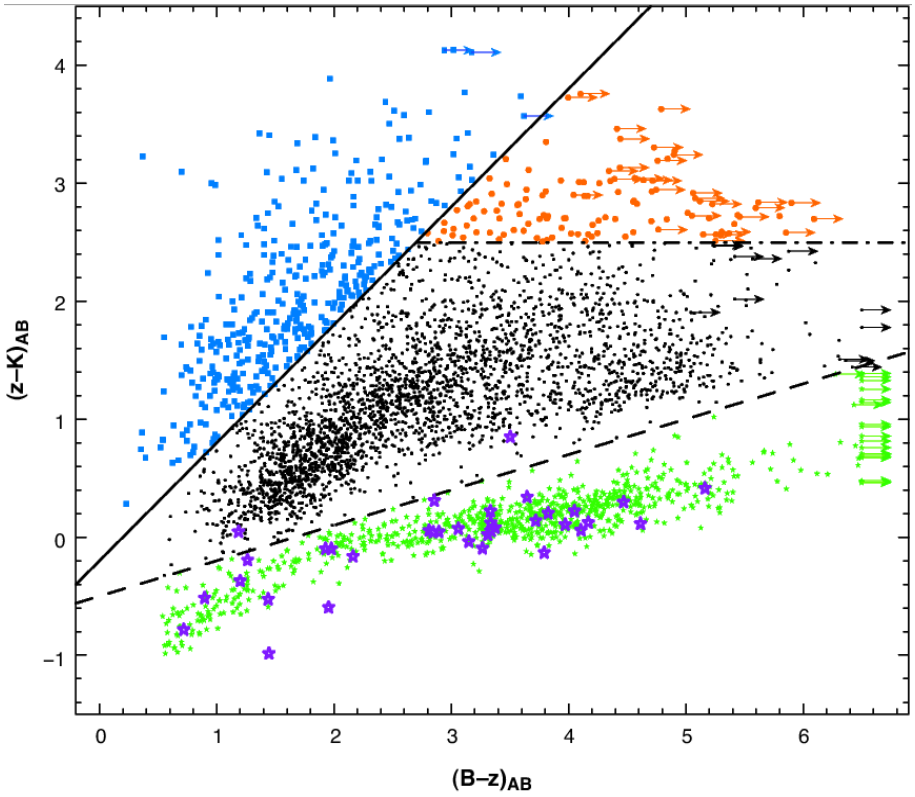


Figure 15: The $BzK$ plot introduced by Daddi et al. (2004) is here shown for objects to a limiting magnitude $K_{\rm Vega} = 20$ from a 320 arcmin$^2$ field (from Kong et al. 2006). Black dots refer to galaxies at $z <\sim 1.4$, blue dots refer to starforming galaxies at $\sim 1.4 < z <\sim 2.5$, orange dots refer to passively evolving galaxies at $\sim 1.4 < z <\sim 2.5$. Green dots are Galactic stars in the same field and purple stars are local stellar standards.

fields in order to improve the statistics and cope with cosmic variance. Finally, the HDF-South optical data were complemented by ultra-deep $JHK$ imaging at the VLT (the FIRES survey, Labbé et al. 2003, Franx et al. 2003), revealing a population of near-IR galaxies with very red colors ($J - K > 2.3$), called distant red galaxies (DRG), a fraction of which may be ETGs at very high redshifts (see below). Compared to HDF-North, its Southern equivalent appeared to be much richer in very red galaxies, e.g., including 7 objects with $(V - H)_{\rm AB} > 3$ and $H_{\rm AB} < 25$ while HDF-North has only one. Clearly, exploring much wider fields compared to HDF's $\sim 5$ arcmin$^2$ field was imperative in order to make any significant progress.

Passive ETGs formed at very high redshift (e.g., $z > 3$) would indeed have very red colors at $z\gtrsim 1$, and thus they should be found among the so-called extremely red objects (ERO), a class defined for having $R - K > 5$ (or similar color cut), and whose characteristics and relation to ETGs have been thoroughly reviewed by McCarthy (2004). Using a much shallower sample than that from the HDF, but one that covers an area $\sim 140$ times wider than it, Daddi et al. (2000) and Firth et al. (2002) showed that EROs are much more abundant than previously found in smaller fields and are much more strongly clustered than generic galaxies to the same limiting magnitude $K \sim 19$. This made them likely candidates for

high-$z$ ETGs, and assuming that $\sim 70\%$ of EROs are indeed ETGs at $z > 1$, Daddi, Cimatti & Renzini (2000) concluded that most field ellipticals were fully assembled by $z \sim 1$. However, Cimatti et al. (2002a) actually found that out of the 30 EROs with secure redshifts and $K < 19.2$, only 50% are passively evolving objects and these are distributed in the redshift interval $0.8 \lesssim z \lesssim 1.3$, while the other 50% is made by highly-reddened, actively star-forming galaxies. Interestingly, precisely 50% among a sample of 129 EROs with $K < 20.2$ have been detected at 24 $\mu$m with Spitzer/MIPS, reinforcing the conclusion that up to one half of EROs are likely to be passive precursors to ETGs (Yan et al. 2004). In fact, the fraction of passive EROs decreases to $\sim 35\%$ on a spectroscopic complete sample to $K = 20$ (Cimatti et al. 2003). Nevertheless, the number density of passive EROs appeared to be broadly consistent with no density evolution of ETGs up to $z \sim 1$, or a modest decrease.

With the COMBO-17 survey Bell et al. (2004b) went a long way toward coping with cosmic variance. With their 5,000 color-selected ETGs up to photometric redshift $z \sim 1.1$, Bell and colleagues were able to construct their rest-frame $B$-band luminosity functions in nine redshift bins ($0.2 < z < 1.1$), and derived the best fit Schechter parameters for them using a fixed value of the faint-end slope, $\alpha = -0.6$. They found that the characteristic luminosity $M^*_{\rm B}$ brightens by $\sim 1.0$ mag between $z = 0.25$ and 1.05, consistent with passive evolution within the errors, and also with the brightening expected from the FP shift ($\Delta \log M/L_{\rm B} = -0.46 \Delta z$), which predicts $\sim 0.9$ mag. At the same time, the normalization factor $\phi^*$ drops by a factor of $\sim 4$, but much of the drop is in the highest redshift bins which may be affected by incompleteness. More robust than either $\phi^*$ or $L^*$ separately, is their product $\phi^* L^*_{\rm B}$ which is proportional to the $B$-band luminosity density, and this is found to be nearly constant up to $z \sim 0.8$. This is at variance with a pure passive-evolution scenario, that would have predicted an increase by a factor of $\sim 2$. Thus, the color of the COMBO-17 red sequence follows nicely the expectation from passive evolution (cf. section 4.2), but the number density of red sequence galaxies does not, and Bell and colleagues concluded that the stellar mass in red sequence galaxies has nearly doubled since $z \sim 1$.

In a major observational effort at the Keck telescope, Faber et al. (2006, DEEP2 project) secured spectroscopic redshifts for $\sim 11,000$ galaxies with $R < 24.1$, and also reanalyzed the COMBO-17 data, finding separate best fit Schechter parameters in various redshift bins up to $z \sim 1.1$. Faber and colleagues emphasize that $\phi^*$ and $M^*$ are partly degenerate in these fits, for which the faint-end slope was fixed at $\alpha = -0.5$. Thus, between $z = 0.3$ and 1.1, $M^*$ brightens by $\sim 0.47$ mag and $\phi^*$ drops by a factor of $\sim 2.5$ for the DEEP2 data, and respectively up by $\sim 0.95$ mag and down by a factor of $\sim 4$ for the COMBO-17 data. Once more, much of the $\phi^*$ drops are confined to the last redshift bin, and emphasis is placed on both DEEP2 and COMBO-17 confirming that the $B$-band luminosity density is nearly constant up to $z \sim 0.8$, along with the implication that the mass density in ETGs has increased, presumably by a factor of $\sim 2$, as estimated by Bell et al. (2004b). Extending the analysis from $z = 0.3$ to $z = 0$ (using SDSS data), Faber an colleagues find $\Delta M^* \sim 1.3$ mag and a drop in $\phi^*$ by a factor of $\sim 4$ between $z = 0$ and 1.1, but caution that much of these changes occur between the $z \sim 0$ survey and their first bin (at $z = 0.3$) at one end, and in the last redshift bin at the other end, where the data are said to be the weakest.

Both in COMBO-17 and DEEP2 the shape of the Schechter function for the

red-sequence galaxies is assumed constant with redshift. As such, by construction this assumption virtually excludes down-sizing, for which ubiquitous indications have emerged both at low as well as high redshift. Indeed, as alluded in Kong et al. (2006) and documented by Cimatti, Daddi & Renzini (2006), COMBO-17 and DEEP2 results can also be read in a different way. Figure 16 shows the evolution of the rest frame $B$-band LF from COMBO-17, with the continuous line being the local LF for red-sequence galaxies from Baldry et al. (2004). The local LF has been shifted according to the brightening derived from the empirical FP shift with redshift for cluster ETGs (i.e., by $\Delta M_{\rm B} = -1.15\Delta z$, coming from $\Delta(M/L_{\rm B}) = -0.46z$ (van Dokkum & Stanford 2003), taken as the empirical template for passive evolution. From Figure 16 it is apparent that the brightest part of the LF is fully consistent with pure passive evolution of the most massive galaxies, whereas the fainter part of the LF (below $\sim L^*$) is progressively depopulated with increasing redshift, an effect that only in minor part could be attributed to incompleteness. Therefore, from these data it appears that virtually all the most massive ETGs have already joined the red sequence by $z \sim 1$, whereas less massive galaxies join it later. This is what one would expect from the down-sizing scenario, as exemplified e.g., in Figure 6, as if down-sizing was not limited to stellar ages (stars in massive galaxies are older), but it would work for the assembly itself, with massive galaxies being the first to be assembled to their full size. Being more directly connected to the evolution of dark matter halos, an apparent antihierarchical assembly of galaxies may provide a more fundamental test of the ΛCDM scenario than the mere down-sizing in star formation.

The slow evolution with redshift of the number density of spectrum-selected bright ETGs was also one of the main results of the K20 survey (Pozzetti et al. 2003), and more recently of the VLT VIMOS Deep Survey (VVDS) where the rest-frame $B$-band LF of ETGs to $I < 24$ is found to be broadly consistent with passive evolution up to $z \sim 1$, with the number density of bright ETGs decreasing by $\sim 40\%$ between $z = 0.3$ and 1.1 (Zucca et al. 2006).

Quite the same scenario, in which the most massive ETGs are already in place at $z \sim 1$ while less massive ones appear later, emerges from the study of the evolution of the stellar mass function for morphologically-selected ETGs in the GOODS fields (Bundy, Ellis & Conselice 2005, Caputi et al. 2006, Franceschini et al. 2006), and especially from the thorough re-analysis by Bundy et al. (2006) of the color-selected ETGs from the DEEP2 survey. No such effect for morphologically-selected ETGs in the GOODS-South field is mentioned in a recent study by Ferreras et al. (2005), who report instead a steep decrease in their number density with redshift. It seems fair to conclude that to fully prove (or disprove) down-sizing in mass assembly, and precisely quantify the effect, one needs to explore the luminosity and mass functions to deeper limits than reached so far, while extending the search to wider areas is needed to overcome cosmic variance. An endeavour of this size requires an unprecedented amount of observing time at virtually all major facilities, both in space and on the ground. The COSMOS project covering 2 square degrees (Scoville 2005) is deliberately targeted to this end, providing public multiwavelength data extending from X rays to radio wavelengths that will allow astronomers to map the evolution of galaxies and AGNs in their large scale structure context, and to derive photometric and spectroscopic redshifts (Lilly 2005) to substantially fainter limits than reached so far. Thus, it will be possible to directly assess the interplay be-

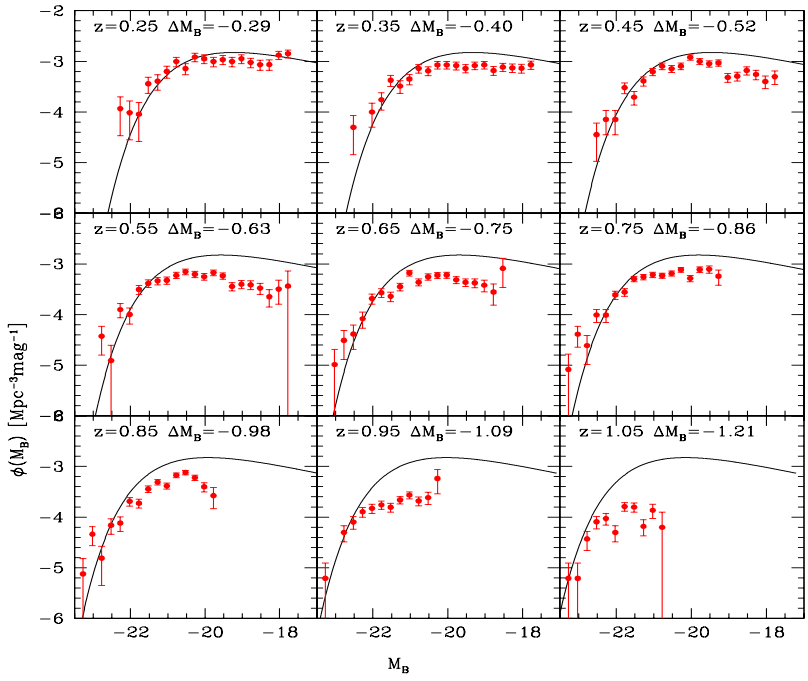


Figure 16: The evolution of the rest-frame $B$-band luminosity function of early-type (red sequence) galaxies from COMBO-17 (Bell et al. 2004) is compared to to the local luminosity function (solid line) from Baldry et al. (2004). The local LF has been shifted in magnitude as indicated in each panel, which corresponds to pure passive evolution as empirically derived from the FP shift of cluster of galaxies ($\Delta M/L_{\rm B} = -0.46z$, van Dokkum & Stanford 2003). Note that there appears to be no number density evolution at the bright end (i.e., for most massive galaxies), whereas at fainter magnitudes there is a substantial decline with redshift of the number density of ETGs. (From Cimatti, Daddi & Renzini 2006.)

tween AGN activity, star-formation onset and quenching, merging, mass growth, and morphological differentiation over the largest presently possible scale, hence promising substantial, perhaps definitive progress in mapping the evolution of ETGs and their progenitors.

It is worth emphasizing that even a low-level of ongoing star formation can make galaxies drop out of our ETG samples, and that theoretical models do not make solid predictions on when star formation is going to cease in a dark matter halo. Therefore, in a broader perspective, what is perhaps more fundamental than the early-type/late-type distinction, is the stellar mass of galaxies and the evolution of the galaxy mass function, irrespective of galaxy type. Several ongoing studies are moving in this directions (e.g., Fontana et al. 2004, Drory et al. 2004, 2005, Bundy, Ellis, & Conselice 2005, Gabasch et al. 2005, Conselice, Blackburne, & Papovich 2005, etc.), but extending the discussion to the general mass assembly of galaxies goes beyond the scope of this review.

## 5 CATCHING ELLIPTICALS IN FORMATION

Immediate precursors for cluster ETGs in the local universe were first identified with a population of blue, star-forming galaxies whose fraction in clusters increases very rapidly with redshift (Butcher & Oemler 1978, 1984, a trend known as the Butcher-Oemler effect), and therefore most such blue, star-forming galaxies had to subside to passive ETGs by $z \sim 0$. Dressler el al. (1997) and Fasano et al. (2000) showed that in clusters up to $z \sim 0.5$ the fraction of true ellipticals is fairly constant, while the fraction of (star-forming) spirals rapidly increases at the expense of the S0's. This was interpreted as evidence that galaxies in clusters that were star-forming spirals at $z \sim 0.5$, have changed their morphology to become passively evolving S0's by $z = 0$, a transformation that may account for much of the Butcher-Oemler effect. In clusters in the same redshift range, a sizable population of ETGs with strong Balmer absorption lines was also identified by Dressler & Gunn (1983), hence called K+A galaxies after the appearance of their spectrum. These ETGs were recognized as poststarburst galaxies, as further documented by Dressler et al. (1999, 2004) and Poggianti et al. (1999).

Thus, the metamorphosis from $z \sim 0.5$ to $z = 0$ of a fraction of cluster galaxies from star forming to passive is well documented by these studies. However, these changes seem to affect more spirals and S0's than true ellipticals, and if the bulk of star formation in ETGs took place at very high redshift, then we need to look further out to catch them in formation. From the low-redshift studies we have learned that ETGs are massive, highly clustered, and had to form the bulk of their stars at $z \gtrsim 1.5-3$ (depending on mass and environment) within a short time interval. Indeed, fast star formation is required by the $\alpha$-overabundance, and by the mere high formation redshift. At $z \sim 3$ the universe is only $\sim 2$ Gyr old, hence forming $\sim 10^{11} M_{\odot}$ of stars in one object between $z = 5$ and $z = 3$ ($\Delta t \sim 1$ Gyr) requires a star-formation rate (SFR) of $\gtrsim 100\, M_{\odot}\mathrm{yr}^{-1}$. Altogether, possible precursors of massive ETGs at low $z$ could be searched among high-$z$ massive, highly clustered, starburst galaxies with very high SFRs ($\gtrsim 100\, M_{\odot}\mathrm{yr}^{-1}$). The rest of this section is dedicated to mentioning the main results in searching for such objects.

Lyman break galaxies (LBGs) were the first ubiquitous population of galaxies to be identified at $z \sim 3$, and their SFRs often in excess of $\sim 100\, M_{\odot}\mathrm{yr}^{-1}$, plus their relatively small size ($R_{\mathrm{e}} \sim 1 - 3$ kpc), made them natural precursors to local bulges and ETGs (e.g., Giavalisco, Steidel, & Macchetto 1996, Steidel et al. 1996, Giavalisco 2002, but see also Giavalisco et al. 1995 for an even earlier attempt to identify a $z = 3.4$ precursor to ETGs). Recently, Adelberger et al. (2005) show that the 3D correlation length ($r_{\circ}$) of LBGs is such to match that of local lesser spheroids ($M \lesssim 10^{11} M_{\odot}$) when the secular increase of $r_{\circ}$ is taken into account. However, Adelberger et al. note that the most massive and most rapidly star forming galaxies at high redshifts are likely to be lost by the Lyman break selection. From Figure 2 we see that local ETGs with $M > 10^{11} M_{\odot}$ include almost 50% of the mass in this kind of galaxies, and $\sim 1/4$ of the total stellar mass at $z = 0$. Therefore, looking at the starforming precursors of the most massive ETGs refers to a major component of the whole galaxy population. Hence the search was not limited to the LBG technique.

Other obvious candidates are the ultraluminous infrared galaxies (ULIRG, Sanders et al. 1988, Genzel & Cesarsky 2000), detected in mm or sub-mm surveys (e.g., Ivison et al. 1998, Lilly et al. 1999), a class defined for their

infrared luminosity ($8-1000\,\mu$m) exceeding $\sim 10^{12}L_\odot$, and whose typical SFRs ($\gtrsim$200 $M_\odot$yr$^{-1}$) well qualify them for being precursors to massive spheroids, as does their very high (stellar) density ensuring that they would "land" on the fundamental plane as star formation subsides (Kormendy& Sanders 1992, Doyon et al. 1994). ULIRGs as ETG in formation are also advocated by Genzel et al. (2001), who from the resolved kinematics for 12 of them argue that typical ULIRGs are likely precursors to intermediate-mass ETGs rather than to giant ellipticals. However, the internal kinematics of one ULIRG at $z = 2.8$ indicates a mass $\gtrsim 3\times10^{11}M_\odot$ (Genzel et al. 2003) making it a likely precursor to a very massive ETG. Blain et al. (2004) note that submillimeter-selected galaxies at $z = 2-3$ appear to be more strongly clustered than LBGs at the same redshifts, which makes them more attractive candidates than LBGs for being the progenitors of the most massive ETGs. Still, their space density falls short by a factor of $\sim 10$ compared to passive EROs at $z \sim 1$, and they could be the main precursors to EROs only if their duty cycle is very short. Nevertheless, Chapman et al. (2005) argue that the sub-mm galaxies may well be the dominant site of massive star formation at $z = 2-3$, once more making them excellent candidates for being ETG in formation.

The survey and characterization of sub-mm galaxies are currently limited by the modest sensitivity and resolution of existing sub-mm facilities, hence optical/near-IR selections are still the most efficient way of identifying large samples of massive star-forming galaxies at high redshift. For the star-forming $BzK$-selected objects, Daddi et al. (2004) estimate $<$SFR$>\simeq 200\,M_\odot$yr$^{-1}$, which is typical of ULIRGs, and most of them are clearly mergers on ACS images. Indeed, out of 131 non-AGN (i.e., non X-ray emitter) star-forming BzKs with $K < 20$ in the GOODS-North field (Dickinson et al. in preparation), 82% were individually detected with Spitzer/MIPS at 24 $\mu$m (Daddi et al. 2005a). Moreover, by stacking the fluxes of the 131 objects ($<z>= 1.9$) from radio to X-rays (i.e., VLA 1.4 GHz, SCUBA 850 and 450 $\mu$m, MIPS 24 $\mu$m, IRAC 8-3.5 $\mu$m, near-IR and optical bands, and Chandra's 0.5-8 keV) Daddi and colleagues showed that the resulting composite SED is an excellent match to that of a template ULIRG with $L_{\rm IR} = 1.7\times10^{12}L_\odot$ and $<$SFR$>\simeq 250\,M_\odot$yr$^{-1}$, in agreement with the typical SFRs derived from the extinction-corrected UV flux. Two of these BzKs have also been detected at 1.2 mm with MAMBO, implying a SFR$\sim 1000\,M_\odot$yr$^{-1}$ (Dannerbauer et al. 2006). So, the BzK selection proves to be an excellent way of finding large numbers of ULIRGs at high redshift, whose space density at $z \sim 2$ ($\sim 1-2\times10^{-4}$Mpc$^{-3}$) is about three orders of magnitudes higher than the local density of ULIRGs, and a factor of 2-3 higher than that at $z = 1$. Moreover, the number of star-forming BzKs with $M > 10^{11}M_\odot$ is close to that of passive BzKs of similar mass, and added together nearly match the space density of massive ETGs at $z = 0$ (Kong et al. 2006). Hence, it is tantalizing to conclude that as star formation subsides in star-forming BzKs the number of passive ETGs will approach their local density. Finally, worth mentioning is that the majority among samples of $J-K > 2.3$ DRGs in the Extended HDF-South field (Webb et al. 2006) and GOODS-South field (Papovich et al. 2006) have been recently detected at 24 $\mu$m with Spitzer/MIPS, indicating that the majority of DRGs are likely to be dusty starburst precursors to ETGs, rather than having already turned into passive ETGs themselves. Moreover, DRGs appear to be distributed over a very broad and nearly flat redshift distribution, from less than 1 to over $\sim 3.5$ (Reddy et al. 2006).

Moderate redshift precursors to local ETGs are not necessarily star-forming. They may also be less massive ETGs that will merge by $z = 0$, an event now called "dry merging". The merger rate since $z \sim 1.2$ has been estimated by Lin et al. (2004) as part of the DEEP2 survey, concluding that only $\sim 9\%$ of present-day $M^*$ galaxies have undergone a major merger during the corresponding time interval. However, Bell et al. (2006) searched for dry merger candidates over the GEMS field, and based on 7 ETG-ETG pairs estimated that each present-day ETG with $M_{\rm v} < -20.5$ has undergone 0.5–1 major dry merger since $z \sim 0.7$. This may be at variance with the estimate based on the 3D two-point correlation function of local ETGs in the overwhelming SDSS database. Indeed, each local ETG is found to have less than 1% probability per Gyr of merging with another ETG, hence the dry merging rate appears to be "lower, much lower than the rate at which ETG-hosting DM halos merge with one another" (Hogg 2006), at least for $z \lesssim 0.36$ (Masjedi et al. 2006).

The history of star formation in ETGs has been deduced from the properties of their passively evolving stellar populations in low and high redshifts galaxies, and we know that ETGs and bulges hold at least $\sim 50\%$ of the stellar mass at $z = 0$. Threfore, it is worth addressing here one last issue, even if only in a cursory way: is such an inferred history of star formation consistent with the direct measurements of the star-formation density and stellar mass density at high redshifts? Based on the estimate that the bulk of stars in spheroids formed at $z \gtrsim 3$, it has been suggested that at least $\sim 30\%$ of all stars (and metals) have formed by $z = 3$ (Renzini 1999). This appears to be at least a factor of $\sim 3$ higher than the direct estimate based on the HDF-North, according to which only $3\% - 14\%$ of today's stars were in place by $z = 3$ (Dickinson et al. 2003). Data from HDF-South give the higher value $10\% - 40\%$ (Fontana et al. 2003), most likely as a result of cosmic variance affecting both HDF fields. Based on the $\sim 10$ times wider field of the K20 survey, $\sim 30\%$ of the stellar mass appears to be in place by $z \sim 2$ (Fontana et al. 2004), but the corrections for incompleteness are large. Drory et al. (2005) find that over the $\sim 200$ arcmin$^2$ area of the combined GOODS-South and FORS Deep Field, $\sim 50\%$, $\sim 25\%$, and at least $\sim 15\%$ of the mass in stars is in place, respectively at $z = 1$, 2, and 3. So, no gross discrepancy has emerged so far between the mass density at $z \sim 3$ as directly measured and as estimated from the fossil evidence at lower redshift. The same holds for the comparison between the star-formation densities as a function of redshift, as inferred from the distribution of stellar ages of ETGs on the one hand, and as directly measured by observations on the other hand (e.g., Madau et al. 1996, Steidel et al. 1999, Giavalisco et al. 2004b). Errors on both sides are still as large as a factor of 2 or 3, but this should rapidly improve thanks to the deep and wide surveys currently under way.

## 6 EPILOGUE

Almost thirty years ago Toomre (1977) remarked that star formation was observed only in galaxy disks, and further that the final state of merging spirals must be something resembling an elliptical galaxy. Thus, merging spirals to form ellipticals at relatively low redshifts became very popular, especially following the success of CDM theories in accounting for the growth of large scale structure from tiny initial perturbations.

However, in the intervening three decades an impressive body of evidence on galaxies at low as well as high redshift has accumulated, that at least in part contradicts Toomre's assumption. While in the local universe most of the star formation is indeed confined to disks; at $z > 1 - 1.5$ most of it appears to take place in starburst galaxies, such as ULIRGs, whose space density is orders of magnitude higher than in the local universe. Moreover, $\sim 50\%$ of all stars seem to have formed at $z \lesssim 1$ (Dickinson et al. 2003), and to have occurred mostly in disks (Hammer et al. 2005), whereas, if the scenario shown in Figure 6 is basically correct, then the bulk of star formation in ETGs took place at much higher redshift. At the risk of some simplification, we can say that the era of ETG/spheroid/elliptical formation was largely finished by $z \sim 1$ (if not before), just when the major build up of disks was beginning (see also Papovich et al. 2005).

The evidence for the stellar populations in ETGs being old, and older in massive galaxies than in less massive ones, has been known for over ten years, along with the evidence for down-sizing and for the anticorrelation of mass and SFR. Theoretical models based on the CDM paradigm have recently incorporated these observational constraints, and have been tuned to successfully reproduce the down-sizing effect in star formation (e.g., De Lucia et al. 2006). In a hierarchical scenario, down-sizing in star formation is indeed natural. Star formation starts firsts in the highest density peaks, which in turn are destined to become the most massive galaxies later on. But until recently models predicted that star formation was continuing all the way to low redshift, as cooling flows were left uncontrasted, thus failing to even produce a red sequence. To get the old and dead massive galaxies we see in nature, such cooling flows (and the accompanying star formation) had to be suppressed in the models, which is now generally accomplished by invoking strong AGN feedback, as first incorporated in ΛCDM simulations by Granato et al. (2001)[2]. Yet, the AGN responsibility in switching off star formation remains conjectural at this time, but we became aware that galaxies and supermassive black holes co-evolve, which means we must understand their formation as one and the same problem.

Baryon physics, including star formation, black hole formation and their feedbacks, is highly nonlinear, and it is no surprise if modelling of galaxy evolution relies heavily on many heuristic algorithms, their parameterization, and trials and errors. Dark matter physics, on the contrary, is extremely simple by comparison. Once DM halos are set into motion, there is nothing preventing them from merging with each other under the sole action of gravity, and growing bigger and bigger "galaxies" in an up-sizing process. Thus, the vindication of the ΛCDM paradigm should be found in observations demonstrating that the biggest, most

[2]See also Ciotti et al. (1991) and Ciotti & Ostriker (1997) for early attempts to suppress cooling flows in ETGs, either with Type Ia supernova feedback alone, or in combination with AGN feedback.

massive galaxies are the first to disappear when going to higher and higher redshifts. This is indeed what has not been seen yet, and actually there may be hints for the contrary.

ACKNOWLEDGMENTS

I thank Ralf Bender, Andrea Cimatti, Emanuele Daddi, Mauro Giavalisco, Laura Greggio, Silvia Pellegrini and Daniel Thomas for a critical reading of the manuscript and for their valuable suggestions. I am indebted to Mariangela Bernardi, Daniel Thomas, and Sperello di Serego Alighieri, for having provided respectively Table 1, Figure 2, and Figure 13, specifically for this paper. Finally, I am very grateful to my Annual Review tutoring editor John Kormendy for his guidance, to Doug Beckner for the final set up of all the figures, and to Roselyn Lowe-Webb for her patience in proof-editing the manuscript.

*Literature Cited*

1. Adelberger KL, Steidel CC, Pettini M, Shapley AE, Reddy NA, et al. 2005. ApJ 619:697
2. Aragón-Salamanca A, Ellis RS, Couch WJ, Carter D. 1993 MNRAS 262:764
3. Arimoto N, Yoshii Y. 1987. A&A 173:23
4. Baldry IK, Galzebrook K, Brinkmann J, Ivezić Z, Lupton LH, et al. 2004. ApJ 600:681
5. Barbuy B, Renzini A. 1992. *The Stellar Populations of Galaxies*, IAU Symp. 149, Dordrecht:Kluwer
6. Barger AJ, Aragón-Salamanca A, Smail I, Ellis, RS, Couch WJ, et al. 1998. ApJ 501:522
7. Barger AJ, Cowie LL, Trentham N, Fulton E, Hu EM, et al. 1999. AJ 117:102
8. Barrientos LF, Lilly SJ. 2003. ApJ 596:129
9. Barrientos LF, Schade D, Lopez-Cruz O. 1996. ApJ 460:89
10. Baum WE. 1959. PASP 71: 106
11. Bell EF, McIntosh DH, Barden M, Wolf C, Caldwell JAR, et al. 2004a. ApJ 600:L11
12. Bell EF, McIntosh DH, Katz N, Weinberg MD. 2003. ApJS 149:289
13. Bell EF, Naab T, McIntosh DH, Somerville RS, Caldwell JAR, et al. 2006. ApJ 640:241
14. Bell EF, Wolf C, Meisenheimer K, Rix H-W, Borgh A, et al. 2004b. ApJ 608:752
15. Bender R, Burnstein D, Faber SM. 1992. ApJ 399:462
16. Bender R, Saglia RP, Ziegler B. 1996. In *The Early Universe with the VLT*, ed. J. Bergeron. Berlin: Springer, p. 105
17. Bender R, Ziegler B, Bruzual G. 1996. ApJ 463:L51
18. Bender R, Saglia RP, Ziegler B, Belloni P, Greggio L, et al. ApJ 493:529
19. Benitez N, Broadhurst T, Bouwens R, Silk J, Rosati P. 1999. ApJ 515:L65
20. Bernardi M, Nichol RC, Sheth RK, Miller CJ, Brinkmann J. 2006, AJ 131:1288
21. Bernardi M, Renzini A, da Costa LN, Wegner C, Alonso MV, et al. 1998. ApJ 508:L143
22. Bernardi M, Sheth RK, Annis J, Burles S, Finkbeiner DP, et al. 2003a. AJ 125:1882
23. Bernardi M, Sheth RK, Annis J, Burles S, Eisenstein DJ, et al. 2003b. AJ 125:1866
24. Bernardi M, Sheth RK, Nichol RC, Schneider DP, Brinkmann J. 2005. AJ 129:61
25. Blain AW, Chapman SC, Smail I, Ivison R. 2004. ApJ 611:725
26. Blakeslee JP, Franx M, Postman M, Rosati P, Holden BP, et al. 2003. ApJ 596:L143
27. Bower G, Lucey JR, Ellis RS. 1992.MNRAS 254:613
28. Bower G, Kodama T, Terlevich A. 1998. MNRAS 299:1193
29. Bower G, Terlevich A, Kodama T, Caldwell N. 1999. ASP Conf. Ser. 163:211
30. Bressan A., Chiosi C, Fagotto F. 1994. ApJS 94:63
31. Bressan A., Chiosi C, Tantalo R. 1996. A&A 311:425
32. Broadhurst T, Bouwens R. 2000. ApJ 530:L53
33. Brown TM, Bowers CW, Kimble RA, Sweigart AV, Ferguson HC. 2000. ApJ 532:308
34. Bruzual G. 1983. ApJ 273:105
35. Bruzual G, Charlot S. 2003. MNRAS 344:1000
36. Bundy K, Ellis RS, Conselice CJ. 2005. ApJ 625:621
37. Bundy K, Ellis RS, Conselice CJ, Taylor JE, Cooper MC, et al. 2006. ApJ In press (astro-ph/0512465)
38. Burstein D, Faber SM, Gaskell CM, Krumm N. 1984. ApJ 287:586

39. Busarello G, Capaccioli M, Capozziello S, Longo G, Puddu E. 1997. A&A 320:415
40. Buson LM, Bertola F, Bressan A, Burstein D, Cappellari M. 2004. A&A 423:965
41. Butcher H, Oemler A. 1978. ApJ 219:18
42. Butcher H, Oemler A. 1984. ApJ 285:426
43. Buzzoni A. 1995. ApJS 98:69
44. Caputi KI, McLure RJ, Dunlop JS, Cirasuolo M, Schael AM. 2006. MNRAS 366:609
45. Chabrier G. 2003. PASP 115:736
46. Chen H-W, Marzke RO. 2004. ApJ 615:603
47. Cimatti A, Daddi E, Cassata P, Pignatelli E, Fasano G, et al. 2003. A&A 412:L1
48. Cimatti A, Daddi E, Mignoli M, Pozzetti L, Renzini A, et al. 2002a. A&A 381:L68
49. Cimatti A, Daddi E, Renzini A 2006. A&A In press (astr-ph/0605353)
50. Cimatti A, Daddi E, Renzini A, Cassata P, Vanzella E, et al. 2004. Nature 430:184
51. Cimatti A, Mignoli M, Daddi E, Pozzetti L, Fontana A, et al. 2002b. A&A 392:395
52. Ciotti L 1997. See da Costa & Renzini, p. 38
53. Ciotti L, D'Ercole A, Pellegrini S, Renzini A. 1991. ApJ 376: 380
54. Ciotti L, Lanzoni B 1997. A&A 321:724
55. Ciotti L, Lanzoni B, Renzini A 1996. MNRAS 282:1
56. Ciotti L, Ostriker JP. 1997. ApJ 487:L10
57. Conselice CJ, Blackburne JA, Papovich C. 2005. ApJ 620:564
58. Cowie LL, Songaila H, Hu EM, Cohen JG. 1996. AJ 112:839
59. da Costa LN, Renzini A. 1997. *Galaxy Scaling Relations*, Berlin:Springer
60. Daddi E, Cimatti A, Pozzetti L, Hoeckstra H, Röttgering HJA, et al. 2000. A&A 361:535
61. Daddi E, Cimatti A, Renzini A. 2000. A&A 362:L45
62. Daddi E, Cimatti A, Renzini A, Fontana A, Mignoli M, et al. 2004. ApJ 617:747
63. Daddi E, Dickinson M. Chary R. Pope A, Morrison G, et al. 2005a. ApJ 631:L13
64. Daddi E, Renzini A, Pirzkal N, Cimatti A, Malhotra S, et al. 2005b. ApJ 626:680
65. Dannerbauer H, Daddi E, Onodera M, Kong X, Röttgering H, et al. 2006. ApJ 637:L5
66. Davies RL, Sadler EM, Peletier RF. 1993. MNRAS 262:650
67. De Lucia G, Poggianti BM, Aragón-Salamanca A, Clowe D, Halliday C, et al. 2004. ApJ 610:L77
68. De Lucia G, Springel V, White SDM, Croton D, Kauffmann G. 2006. MNRAS 366:499
69. De Propris R, Stanford SA, Eisenhardt PR, Dickinson M, Elston R. 1999. AJ 118:719
70. Dickinson M. 1997. See da Costa & Renzini, p. 215
71. Dickinson M, Papovich C, Ferguson HC, Budavari T. 2003. ApJ 587:25
72. di Serego Alighieri S, Vernet J, Cimatti A, Lanzoni B, Cassata P, et al. 2005. A&A 442:125
73. Djorgovski S, Davis M. 1987. ApJ 313:59
74. Doyon R, Wells M, Wright GS, Joseph RD, Nadeau D, James PA. ApJ 437:L23
75. Dressler A, Gunn, J. 1983. ApJ 270:7
76. Dressler A, Gunn, J. 1990. in *The Universe of Galaxies*, p. 200. San Francisco:ASP
77. Dressler A, Lynden-Bell D, Burnstein D, Davies RL, Faber SM, et al. 1987. ApJ 313:42
78. Dressler A, Oemler G, Couch WJ, Smail I, Ellis RS, et al. 1997. ApJ 490:577
79. Dressler A, Oemler G, Poggianti B, Smail I, Trager S, et al. 2004. ApJ 617:867
80. Dressler A, Smail I, Poggianti B, Butcher HR, Couch WJ, et al. 1999. ApJS 122:51
81. Driver SP, Fernandez-Soto A, Couch WJ, Odewahn SC, Windorst RA, et al. 1998. ApJ 496:L93
82. Drory N, Bender R, Feulner G, Hopp U, Maraston C, et al. 2004. ApJ 608:742
83. Drory N, Feulner G, Bender R, Botzler CS, Hopp U, et al. 2001. MNRAS 325:550
84. Drory N, Salvato M, Gabasch A, Bender R, Hopp U, et al. 2005. ApJ 619:L131
85. Dunlop J, Peacock J, Spinrad H, Dey A, Jimenez R, et al. 1996. Nature 381:581
86. Eggen OJ, Lynden-Bell D, Sandage AR. 1962. ApJ 136: 748
87. Eisenstein DJ, Hogg DW, Fukugita M, Nakamura O, Bernardi M, et al. 2003. ApJ 585:694
88. Ellis RS, Colless M, Broadhurst T, Heyl J, Glazebrook K. 1996. MNRAS 280:235
89. Ellis RS, Smail I, Dressler A, Couch WJ, Oemler A, et al. 1997. ApJ 483:582
90. Faber SM. 1972. A&A 20:361
91. Faber SM, Jackson R. 1976. ApJ 204:668
92. Faber SM, Willmer CNA, Wolf C, Koo DC, Weiner BJ, et al. 2006. ApJ In press (astro-ph/0506044)
93. Faber SM, Worthey G, Gonzales JJ. 1992. See Barbuy & Renzini 1992, p. 255
94. Falcon-Barroso J, Peletier RF, Balcells M. 2002. MNRAS 335:741

95. Fasano G, Cristiani S, Arnouts S, Filippi M. 1998. AJ 115:1400
96. Fasano G, Poggianti B, Couch WJ, Bettoni D, Kjærgaard P, et al. 2000. ApJ 542:673
97. Ferreras I, Lisker T, Carollo CM, Lilly S, Mobasher B. 2005. ApJ 635:243
98. Feulner G, Gabasch A, Salvato M, Drory N, Hopp U, et al. 2005. ApJ 633:L9
99. Fioc M, Rocca Volmerange B. 1997. A&A 326:950
100. Firth AE, Somerville RS, McMahon RG, Lahav O, Ellis RS, et al. 2002. MNRAS 332:617
101. Fontana A, Donnarumma I, Vanzella E, Giallongo E, Menci N, et al. 2003. ApJ 594:L9
102. Fontana A, Pozzetti L, Donnarumma I, Renzini A, Cimatti A, et al. 2004. A&A 424:23
103. Franceschini A, Rodighiero G, Cassata P, Berta S, Vaccari M, et al. 2006. A&A In press (astro-ph/0601003)
104. Franceschini A, Silva L, Fasano G, Granato L, Bressan A, et al. 1998. ApJ 506:600
105. Franx M, Labbé I, Rudnick G, van Dokkum PG, Daddi E, et al. 2003. ApJ 587:L79
106. Fukugita M, Hogan CJ, Peebles PJE. 1998. ApJ 503:518
107. Gabasch A, Hopp U, Feulner G, Bender R, Seitz S, et al. 2006. A&A 448:101
108. Gavazzi G. 1993. ApJ 419:469
109. Gavazzi G, Pierini D, Boselli A. 1996. A&A 312:397
110. Gebhardt K, Faber SM, Koo DC, Im M, Simard L, et al. 2003. ApJ 597:239
111. Genzel R, Baker AJ, Tacconi LJ, Lutz D, Cox P, et al. 2003. ApJ 584:633
112. Genzel R, Cesarsky C. 2000. ARA&A 38:761
113. Genzel R, Tacconi LJ, Rigopoulou D, Lutz D, Tecza M .2001. ApJ 563:527
114. Giavalisco M. 2002. ARA&A 40:579
115. Giavalisco M, Dickinson M, Ferguson HC, Ravidranath S, Kretchmer C, et al. 2004b. ApJ 600:L103
116. Giavalisco M, Ferguson HC, Koekemoer AM, Dickinson M, Alexander DM, et al. 2004a. ApJ 600:L93
117. Giavalisco M, Macchetto FD, Madau P, Sparks WB. 1995. ApJ 441:L13
118. Giavalisco M, Steidel CC, Macchetto FD. 1996. ApJ 470:194
119. Gladders MD, Lopez-Crus O, Tee HKC, Kodama T. 1998. ApJ 501:577
120. Glazebrook K, Abraham RG, McCarthy PJ, Savaglio S, Chen H-S, et al. Nature 430:181
121. González Delgado RM, Cerviño M, Martins LP, Leitherer C, Hauschildt PH. 2005. MNRAS 357:945
122. Gorgas J, Efstathiou G, Aragón-Salamanca A. 1990. MNRAS 245:217 .
123. Granato GL, Silva L, Monaco P, Panuzzo P, Salucci P, et al. 2001. MNRAS 324:757
124. Greggio L. 1997. MNRAS 285:151
125. Greggio L, Renzini A. 1990. ApJ 364:35
126. Gunn JE, Stryker LL, Tinsley BM. 1981. ApJ 249:48
127. Hammer F, Flores H, Elbaz D, Zheng XZ, Liang YC, et al. 2005. A&A 430:115
128. Hogg D. 2006. In *The Fabulous Destiny of Galaxies: Bridging Past and Present*, ed. V Le Brun, A Mazure, S Arnouts, & D Burgarella. Paris:Edition Frontieres, In press (astro-ph/0512029)
129. Holden BP, Blakeslee JP, Postman M, Illingworth GD, Demarco R. 2005a. ApJ 626:809
130. Holden BP, Stanford SA, Eisenhardt P, Dickinson M. 2004. AJ 127:2484
131. Holden BP, van der Wel A, Franx M, Illingworth GD, Balkeslee JP, et al. 2005b. ApJ 620:L83
132. Hubble EP 1936. *The Realm of the Nebulae* (New Haven: Yale Univ. Press)
133. Im M, Griffiths RE, Ratnatunga KU, Sarajedini VL. 1996. ApJ 461:L79
134. Im M, Griffiths RE, Naim A, Ratnatunga KU, Roche N, et al. 1999. ApJ 510:82
135. Ivison RJ, Smail I, Le Borgne J-F, Blain AW, Kneib J-P, et al. 1998. MNRAS 298:583
136. Jablonka P, Martin P, Arimoto N. 1996. AJ 112:1415
137. Jørgensen I. 1997. MNRAS 288:161
138. Jørgensen I. 1999. MNRAS 306:607
139. Jørgensen I. Chiboucas K, Flint K, Bergmann M, Barr J, et al. 2006. ApJ 639:L9
140. Jørgensen I, Franx M, Kjærgaard P. 1995. MNRAS 276:1341
141. Jørgensen I, Franx M, Kjærgaard P. 1996. MNRAS 280:167
142. Juneau S, Glazebrook K, Crampton D, McCarthy PJ, Savaglio S, et al. 2005. ApJ 619:L135
143. Kauffmann G, Charlot S, White SDM. 1996. MNRAS 283:L117
144. Kauffmann G, Heckman TM, White SDM,Charlot S, Tremonti C, et al. 2003. MNRAS 341:54
145. Kelson DD, Illingworth GD, Franx M, van Dokkum PG. 2001. ApJ 552:L17

146. Kelson DD, Illingworth GD, van Dokkum PG, Franx M. 2000. ApJ 531:184
147. Kelson DD, van Dokkum PG, Franx M, Illingworth GD, Fabricant D. 1997. ApJ 478:L13
148. Kochanek CS, Impey CDE, Lehar J, McLeod BA, Rix H-W, et al. 2000. ApJ 543:131
149. Kodama T, Arimoto N. 1997. A&A 320:41
150. Kodama T, Arimoto N, Barger AJ, Aragón-Salamanca A. 1998. A&A 334:99
151. Kodama T, Bower R. 2003. MNRAS 346:1
152. Kodama T, Yamada T, Akiyama M, Aoki K, Doi M, et al. 2004. MNRAS 350:1005
153. Kong X, Daddi E, Arimoto N, Renzini A, Broadhurst T, et al. 2006. ApJ 638:72
154. Koo DC, Datta S, Willmer CNA, Simard L, Tran K-V, et al. 2005. ApJ 634:L5
155. Kormendy J. 1977. ApJ 218,333
156. Kormendy J, Kennicutt RCJr. 2004. ARA&A 42:603
157. Kormendy J, Sanders DB. 1992. ApJ 390:L93
158. Kuijken K, Rich RM. 2002. AJ 124:2054
159. Kuntschner H, Davies RL. 1998. MNRAS 295:L29
160. Kuntschner H, Lucey RJ, Smith RJ, Hudson MJ, Davies RL 2001. MNRAS 323:615
161. Labbé I, Franx M, Rudnick G, Rix H-W, Moorwood A, et al. 2003. AJ 125:1117
162. Larson RB. 1974. MNRAS 166:585
163. Lidman C, Rosati P, Demarco R, Nonino M, Maineri V. 2004. A&A 416:829
164. Lilly SJ. 2005. *The Messenger*, 121:42
165. Lilly SJ, Eales SA, Gear WKP, Hammer F, Le Fèvre O, et al. 1999. ApJ 518:641
166. Lilly SJ, Le Fèvre O, Crampton D, Tresse L. 1995a. ApJ 455:50
167. Lilly SJ, Tresse L, Hammer F, Crampton D, Le Fèvre O. 1995b. ApJ 455:108
168. Lin L, Koo DC, Willmer CNA, Patton DR, Conselice CJ, et al. 2004. ApJ 617:L9
169. Madau P, Ferguson HC, Dickinson M, Giavalisco M, Steidel CC, et al. 1996. MNRAS 283:1388
170. Maraston C. 1998. MNRAS 300:872
171. Maraston C. 2005. MNRAS 362:799
172. Maraston C, Greggio L, Renzini A, Ortolani S, Saglia RP, et al. 2003. A&A 400:823
173. Maraston C, Thomas D. 2000. ApJ 541:126
174. Masjedi M, Hogg DW, Cool RJ, Eisenstein DJ, Blanton MR, et al. 2006. ApJ In press (astro-ph/0512166)
175. McCarthy PJ. 2004. ARA&A 42:477
176. McCarthy PJ, Le Borgne D, Crampton D, Chen H-W, Abraham R, et al. 2004. ApJ 614:L9
177. McIntosh DH, Bell EF, Rix H-W, Wolf C, Heymans C, et al. 2005. ApJ 632:191
178. Mobasher B, Dickinson M, Ferguson HC, Giavalisco M, Wiklind T, et al. 2005. ApJ 635:832
179. Mobasher B, Guzmán R, Aragón-Salamanca A, Zepf S. 1999. MNRAS 304:225
180. Mullis CR, Rosati P, Lamer G, Böhringer H, Schwope A, et al. 2005. ApJ 623:L85
181. Nelan JE, Smith RJ, Hudson MJ, Wegner GA, Lucey JR, et al. 2005. ApJ 632:137
182. Nelson AE, Gonzalez AH, Zaritsky D, Dalcanton JJ. 2001. ApJ 563:629
183. Norman CA, Renzini A, Tosi M. 1986 *Stellar Populations*, Cambridge:CUP
184. O'Connell RW. 1980. ApJ 236:430
185. O'Connell RW. 1986. See Norman, Renzini & Tosi 1986, p. 167
186. Ortolani S, Renzini A, Gilmozzi R, Marconi G, Barbuy B, et al. 1995. Nature 377:701
187. Pahre MA, de Carvalho RR, Djorgovski SG, 1998. AJ 116:1606
188. Pahre MA, Djorgovski SG, de Carvalho RR. 1995. ApJ 453:L17
189. Pahre MA, Djorgovski SG, de Carvalho RR. 1996. ApJ 456:L79
190. Pahre MA, Djorgovski SG, de Carvalho RR. 1998. AJ 116:1591
191. Papovich C, Dickinson M, Giavalisco M, Conselice CJ, Ferguson HC. 2005. ApJ 631:101
192. Papovich C, Moustakas LA, Dickinson M, Le Floc'h E, Rieke GH, et al. 2006. ApJ 640:92
193. Pasquali A, Ferreras I, Panagia N, Daddi E, Malhotra S, et al. 2006. ApJ 636:115
194. Peletier RF 1989. PhD Thesis, Rijksuniversiteit Gronongen
195. Peletier RF, Balcells M, Davies RL, Andreakis Y, Vazdekis A, et al. 1999. MNRAS 310:703
196. Persic M, Salucci P. 1992. MNRAS 258:14p
197. Poggianti BM, Bridges TJ, Mobasher B, Carter D, Doi M, et al. 2001. ApJ 562:689
198. Poggianti B, Smail I, Dressler A, Couch WJ, Berger AJ, et al. 1999. ApJ 518:576
199. Popesso P, Böhringer H, Romaniello M, Voges W. 2005, A&A 433:415
200. Pozzetti L, Cimatti A, Zamorani G, Daddi E, Menci N, et al. 2003. A&A 402:837
201. Prugniel Ph, Maubon G, Simien F. 2001. A&A 366:68
202. Prugniel Ph, Simien F. 1996. A&A 309:749

203. Rakos KD, Schombert JM. 1995. ApJ 439:47
204. Reddy NA, Erb DK, Steidel CC, Shapley AE, Adelberger KL, et al. 2005. ApJ 633:748
205. Reddy NA, Steidel CC, Fadda D, Yan L, Pettini M, et al. 2006. ApJ In press (astro-ph/0602596)
206. Renzini A. 1986. See Norman, Renzini & Tosi, p. 213
207. Renzini A. 1992. See Barbuy & Renzini 1992, p. 325
208. Renzini A. 1999. In *The Formation of Galactic Bulges*, ed. CM Carollo, HC Ferguson, & RFG Wyse. Cambridge:CUP, 9
209. Renzini A. 2005. In *The Initial Mass Function 50 Years Later*, ed. E Corbelli, F Palla & H Zinnecker. Dordrecht:Springer, p. 221
210. Renzini A, Ciotti L. 1993. ApJ 416:L49
211. Rix H-W, Barden M, Beckwith SVW, Bell EF, Borch A, et al. 2004. ApJS 152:163
212. Rix H-W, de Zeeuw PT, Cretton N, van der Marel RP, Carollo M. 1997. ApJ 488:702
213. Rodighiero G, Franceschini A, Fasano G. 2001. MNRAS 324:491
214. Rosati P, della Ceca R, Norman C, Giacconi R. 1998. ApJ 492:L21
215. Rusin D, Kochanek CS. 2005. ApJ 623:666
216. Sandage A. 2005. ARA&A 43:581
217. Sandage A, Visvanathan N. 1978a. ApJ 223:707
218. Sandage A, Visvanathan N. 1978b. ApJ 225:742
219. Sanders DB, Soifer BT, Elias JH, Madore BF, Matthews K. 1988. ApJ 325:74
220. Saracco P, Longhetti M, Severgnini P, Della Ceca R, Braito V, et al. 2005. MNRAS 357:L40
221. Schade D, Carlberg RG, Yee HKC, Lopez-Cruz O, Ellingson E. 1996. ApJ 464:L63
222. Schade D, Barrientos LF, Lopez-Cruz O. 1997. ApJ 477,L17
223. Schade D, Lilly SJ, Crampton D, Ellis RS, Le Fèvre O, et al. 1999. ApJ 525:31
224. Schechter PL, Dressler A. 1987. AJ 94:563
225. Scodeggio M, Gavazzi G, Biesole E, Pierini D, Boselli A. 1998. MNRAS 301:1001
226. Scodeggio M, Gavazzi G, Franzetti P, Boselli A, Zibetti S, et al. 2002. A&A 384:812
227. Scoville N. 2005. In *Multiwavelength Mapping of Galaxy Formation and Evolution*, ed. A Renzini & R Bender. Berlin:Springer-Verlag, p. 330
228. Spinrad H, Dey A, Stern D, Dunlop J, Peacock J, et al. 1997. ApJ 484:581
229. Stanford SA, Dickinson M, Postman M, Ferguson HC, Lucas RA, et al. 2004. AJ 127:131
230. Stanford SA, Eisenhardt PR, Dickinson M. 1998. ApJ 492:461
231. Stanford SA, Eisenhardt PR, Brodwin M, Gonzalez AH, Stern D, et al. 2005. ApJ 634:L129
232. Steidel CC, Giavalisco M, Pettini M, Dickinson M, Adelberger K. 1996. ApJ 462:17
233. Steidel CC, Adelberger KL, Giavalisco M, Dickinson M, Pettini M. 1999. ApJ 519:1
234. Stephens AW, Frogel JA, DePoy DL, Freedman W, Gallart C, et al. 2003. AJ 125:2473
235. Strazzullo V, Rosati P, Stanford SA, Lidman C, Nonino M, et al. 2006. A&A 450:909
236. Tanaka M, Kodama T, Arimoto N, Okamura S, Umetsu K, et al. 2005. MNRAS 362:268
237. Tantalo R, Chiosi C, Bressan A, Fagotto F. 1996. A&A 311:361
238. Thomas D 1999. MNRAS 306:655
239. Thomas D, Davies RL. 2006. MNRAS 366:510
240. Thomas D, Greggio L, Bender R. 1999. MNRAS 302:537
241. Thomas D, Maraston C, Bender R. 2003. MNRAS 339:897
242. Thomas D, Maraston C, Bender R, Mendez de Oliveira C. 2005. ApJ 621:673
243. Tinsley BM. 1980. *Fund. Cosmic Phys.* 5:287
244. Tinsley BM, Gunn JE. 1976. ApJ 203:52
245. Toft S, Soucail G, Hjorth J. 2003. MNRAS 344:337
246. Toft S, Maineri V, Rosati P, Lidman C, Demarco R, et al. 2004. A&A 422:29
247. Toomre A. 1977. In *Evolution of Galaxies and Stellar Populations*, ed. BM Tinsley & RB Larson. New Haven:Yale University Observatory, p. 401
248. Totani T, Yoshii Y. 1998. ApJ 501:L177
249. Trager SC, Faber SM, Worthey G, Gonzales JJ. 2000. AJ 120:165
250. Treu T, Ellis RS, Liao TX, van Dokkum PG. 2005a. ApJ 622:L5
251. Treu T, Ellis RS, Liao TX, van Dokkum PG, Tozzi P, et al. 2005b. ApJ 633:174
252. Treu T, Stiavelli M, Casertano S, Møller P, Bertin G. 1999. MNRAS 308:1037
253. Treu T, Stiavelli M, Bertin G, Casertano S, Moller P. 2001. MNRAS 326:237
254. Treu T, Stiavelli M, Casertano S, Moller P, Bertin G. 2002. ApJ 564:L13
255. Trujillo I, Burkert A, Bell EF. 2004. ApJ 600:L39
256. van der Wel A, Franx M, van Dokkum PG, Rix H-W. 2004. ApJ 601:L5

257. van der Wel A, Franx M, van Dokkum PG, Rix H-W, Illingworth GD, Rosati P. 2005a. ApJ 631:145
258. van der Wel A, Franx M, van Dokkum PG, Huang J, Rix H-W, et al. 2005b. ApJ 636:L21
259. van Dokkum PG, Ellis RS. 2003. ApJ 592:L53
260. van Dokkum PG, Franx M. 1996. MNRAS 281:985
261. van Dokkum PG, Franx M, Kelson DD, Illingworth GD. 1998. ApJ 504:L17
262. van Dokkum PG, Franx M, Kelson DD, Illingworth GD. 2001. ApJ 553:L39
263. van Dokkum PG, Franx M, Fabricant D, Illingworth GD, Kelson DD. 2000. ApJ 541:95
264. van Dokkum PG, Stanford SA. 2003 ApJ 585:78
265. Vazdekis A, Cenarro AJ, Gorgas J, Cardiel N, Peletier RF. 2003. A&A 340:1317
266. Vázques GA, Leitherer C. 2005. ApJ 621: 717
267. Visvanathan N, Sandage A. 1977. ApJ 216:214
268. Webb TMA, van Dokkum PG, Egami E, Fazio G, Franx M, et al. 2006. ApJ 636:L17
269. Weiss A, Peletier RF, Matteucci F. 1995. A&A 296:73
270. Wheeler JC, Sneden C, Truran JWJr. 1989. ARA&A 27:279
271. White SDM, Rees MJ. 1978. MNRAS 183:341
272. Williams RE, Blacker B, Dickinson M, Dixon WVD, Ferguson HC, et al. 1996. AJ 112:1335
273. Wolf C, Meisenheimer K, Rix H-W, Borch A, Dye S, et al. 2003. A&A 401:73
274. Worthey G. 1994. ApJS 95:107
275. Worthey G, Faber SM, Gonzales JJ. 1992. ApJ 398:69
276. Worthey G, Trager SC, Faber SM. 1995. ASP Conf. Ser. 86:203
277. Wuyts S, van Dokkum PG, Kelson DD, Franx M, Illingworth GD. 2004. ApJ 605:677
278. Yamada T, Kodama T, Akiyama M, Furusawa H, Iwata I, et al. 2005. ApJ 634:861
279. Yan H, Dickinson M, Eisenhardt PRM, Ferguson HC, Grogin NA, et al. 2004. ApJ 616:63
280. Yan L, Choi PI, Fadda D, Marleau FR, Soifer BT, et al. 2004. ApJS 154:75
281. Zepf SE. 1997. Nature 390:377
282. Ziegler BL, Saglia RP, Bender R, Belloni P, Greggio L, et al. 1999. A&A 346:13
283. Ziegler BL, Bender R. 1997 MNRAS 291:527
284. Zoccali M, Renzini A, Ortolani S, Greggio L, Saviane L, et al. 2003. A&A 399:931
285. Zucca E, Ilbert O, Bardelli S, Tresse L, Zamorani G, et al. 2006. A&A In press (astro-ph/0506393)